Published December 1, 2008

Genome-wide analysis reveals a cell cycle–dependent mechanism controlling centromere propagation

Sylvia Erhardt,[1,2,4] Barbara G. Mellone,[1,2] Craig M. Betts,[3] Weiguo Zhang,[1,2] Gary H. Karpen,[1,2] and Aaron F. Straight[3]

[1]Department of Genome Dynamics, Lawrence Berkeley National Laboratory and [2]Department of Molecular and Cell Biology, University of California, Berkeley, Berkeley, CA 94720
[3]Department of Biochemistry, Stanford Medical School, Stanford, CA 94305
[4]Zentrum für Molekulare Biologie, Universität Heidelberg, D-69120 Heidelberg, Germany

Centromeres are the structural and functional foundation for kinetochore formation, spindle attachment, and chromosome segregation. In this study, we isolated factors required for centromere propagation using genome-wide RNA interference screening for defects in centromere protein A (CENP-A; centromere identifier [CID]) localization in *Drosophila melanogaster*. We identified the proteins CAL1 and CENP-C as essential factors for CID assembly at the centromere. CID, CAL1, and CENP-C coimmunoprecipitate and are mutually dependent for centromere localization and function. We also identified the mitotic cyclin A (CYCA) and the anaphase-promoting complex (APC) inhibitor RCA1/Emi1 as regulators of centromere propagation. We show that CYCA is centromere localized and that CYCA and RCA1/Emi1 couple centromere assembly to the cell cycle through regulation of the fizzy-related/CDH1 subunit of the APC. Our findings identify essential components of the epigenetic machinery that ensures proper specification and propagation of the centromere and suggest a mechanism for coordinating centromere inheritance with cell division.

Introduction

Faithful chromosome segregation during mitosis and meiosis is essential for the proper inheritance of the genome. During cell division, chromosomes attach to the spindle through a unique chromosomal structure termed the kinetochore. Kinetochores monitor proper chromosome attachment to the spindle through the mitotic checkpoint and couple spindle and motor protein forces to move chromosomes in prometaphase and anaphase (Cleveland et al., 2003). Centromeres are specialized regions of the chromosome that serve as the structural and functional foundation for kinetochore formation. Centromeric DNA sequences are not evolutionarily conserved, and in most eukaryotes, specific DNA sequences are neither necessary nor sufficient for centromere formation. Thus, centromere formation is thought to be epigenetically controlled through chromatin (Carroll and Straight, 2006).

An excellent candidate for an epigenetic mark that specifies centromere identity is the centromere protein A (CENP-A) family of centromere-specific histone H3 variants (Cleveland et al., 2003). CENP-A is present at centromeres throughout the cell cycle and is essential for the recruitment of kinetochore proteins, establishment of spindle attachments, and normal chromosome segregation in all eukaryotes, which is consistent with it functioning as the foundation for the kinetochore (Carroll and Straight, 2006). Furthermore, CENP-A mislocalization to noncentromeric regions produces functional ectopic kinetochores, suggesting that CENP-A chromatin is sufficient for centromere formation (Heun et al., 2006).

Despite the central role played by CENP-A in kinetochore assembly and function, little is known about the mechanisms that regulate its deposition specifically into centromeric chromatin.

S. Erhardt, B.G. Mellone, and C.M. Betts contributed equally to this paper.

Correspondence to Aaron F. Straight: astraigh@stanford.edu

B.G. Mellone's present address is Dept. of Molecular and Cell Biology, University of Connecticut, Storrs, CT 06269.

Abbreviations used in this paper: APC, anaphase-promoting complex; β-ME, β-mercaptoethanol; BTP, bromothenylpteridine; CENP, centromere protein; CID, centromere identifier; CLD, CID localization deficient; CYCA, cyclin A; DOTAP, 1,2-dioleoyl-3-trimethylammonium-propane; dsRNA, double-stranded RNA; FZR, FZY related; FZY, fizzy; IF, immunofluorescence; LAP, localization and purification; LPC, leupeptin, pepstatin, and chymostatin; Rod, rough deal; TMR*, tetramethyl rhodamine*.

The online version of this article contains supplemental material.

Supplemental Material can be found at:
http://jcb.rupress.org/content/suppl/2008/12/01/jcb.200806038.DC1.html

The Rockefeller University Press $30.00
J. Cell Biol. Vol. 183 No. 5 805–818
www.jcb.org/cgi/doi/10.1083/jcb.200806038

Published December 1, 2008

In *Schizosaccharomyces pombe*, mutations in Mis6 cause loss of Cnp1/CENP-A (Takahashi et al., 2000) from centromeres. The vertebrate Mis6 homologue CENP-I promotes proper localization of newly synthesized CENP-A but is not essential for maintaining previously assembled CENP-A (Okada et al., 2006). Mis16, the *S. pombe* homologue of the *Drosophila melanogaster* p55 subunit of CAF1 (chromatin assembly factor 1) and RbAp46/48 (human retinoblastoma-associated protein 46 and 48), is necessary for CENP-A localization in fission yeast and human cells (Hayashi et al., 2004). The *Drosophila* p55 protein facilitates CENP-A nucleosome assembly in vitro (Furuyama et al., 2006), although the specificity of this reaction for CENP-A is unknown. In fission yeast, another histone chaperone, Sim3, is required for Cnp1/CENP-A deposition at centromeres; however, Sim3 also acts as a chaperone for histone H3, so it is unlikely to provide centromere specificity (Dunleavy et al., 2007).

Currently, the best candidate proteins for regulating the specificity of CENP-A assembly in eukaryotes are *S. pombe* Mis18 and its homologues and binding partners in metazoans (Mis18-α, Mis18-β, and M18BP1/KNL2). Depletion of these proteins in *S. pombe*, *Caenorhabditis elegans*, or human cells results in a failure to incorporate CENP-A at centromeres (Hayashi et al., 2004; Fujita et al., 2007; Maddox et al., 2007). In human cells, these proteins only localize to centromeres during late anaphase to telophase/G1 (Fujita et al., 2007; Maddox et al., 2007). Recent data demonstrating that human CENP-A assembly occurs between telophase and the following G1 and that the *Drosophila* centromere identifier (CID) assembles into the centromere during anaphase (Jansen et al., 2007; Schuh et al., 2007) suggest that activity or removal of the Mis18 complex and mitotic exit may be necessary for centromere formation. However, it is unclear whether known centromere-localized factors regulate CENP-A transcription, translation, nuclear import, chromatin assembly, or maintenance. The identification of factors required for CENP-A localization, without bias for a particular model or biological process, is a strategy that is likely to provide new insights. In this study, we report a genome-wide RNAi screen that identified new factors required for *Drosophila* CID localization to centromeres. This screen revealed significant interdependence between novel and known CENPs for centromere assembly and a novel link between centromere propagation and the cell cycle machinery.

Results

Genome-wide screen for CID localization–deficient (CLD) genes

The generation of double-stranded RNA (dsRNA) collections homologous to ∼24,000 genes and predicted genes in the *Drosophila* genome (Kiger et al., 2003) allowed us to perform a genome-wide RNAi screen to identify factors required for normal centromere localization of CID (Fig. S1, available at http://www.jcb.org/cgi/content/full/jcb.200806038/DC1; see Materials and methods). We directly screened for loss of CID by immunofluorescence (IF) after dsRNA depletion, allowing rapid, unbiased identification of genes that specifically affected centromere propagation rather than relying on an indirect phenotype such as chromosome missegregation or cell lethality.

We have focused detailed experiments on the four CLD genes that when depleted displayed the strongest levels of CID loss from centromeres (Fig. 1 A and Fig. S1 B). The CLD1 gene encodes the *Drosophila* homologue of the essential CENP-C (Heeger et al., 2005). Centromere localization of CENP-C depends on CENP-A in many eukaryotes (Carroll and Straight, 2006), but in this study, we observe that CENP-A and CENP-C are reciprocally dependent for centromere localization. CLD2 is encoded by the CG5148 gene and was recently identified as CAL1 in a screen for mitotic defects in *Drosophila* tissue culture cells (Goshima et al., 2007). CAL1 contains a putative ubiquitin interaction domain, and homology searching identified clear homologues in drosophilids (Fig. S2, available at http://www.jcb.org/cgi/content/full/jcb.200806038/DC1; Clark et al., 2007) but not in other eukaryotes. Interestingly, CLD3 encodes the *Drosophila* cyclin A (CYCA) protein, and CLD4 encodes the regulator of CYCA, RCA1 (Emi1 in vertebrates; Lehner and O'Farrell, 1989; Dong et al., 1997; Machida and Dutta, 2007). Although mitotic cyclins have recently been localized to centromeres (Bentley et al., 2007; Nickerson et al., 2007), neither CYCA nor RCA1 has been implicated in centromere assembly or maintenance. RCA1 protects CYCA from degradation by inhibiting the fizzy (FZY)-related (FZR)/CDH1 anaphase-promoting complex (APC [$APC^{FZR/CDH1}$]; Grosskortenhaus and Sprenger, 2002), suggesting that loss of CID after RCA1 depletion is the result of premature CYCA degradation.

Localization and dynamics of CLD proteins

To determine the localization of CLD proteins, we analyzed the distributions of GFP-CLD fusions in live and fixed *Drosophila* S2 cells (Fig. 1 B and Fig. S3 A, available at http://www.jcb.org/cgi/content/full/jcb.200806038/DC1) and confirmed localization of CYCA and CENP-C by antibody staining in untransfected cells (Fig. S3 A). We performed time-lapse analysis of living cells stably expressing GFP-tagged proteins to determine the dynamics of CLD proteins during the cell cycle (Fig. 1 B and Videos 1–5). As previously reported, CENP-C colocalized with CID throughout the cell cycle (Fig. S3 A and Video 2; Heeger et al., 2005). CYCA was recently shown to localize to centromeres in mouse spermatocytes during late diplotene and prometaphase of meiosis I (Nickerson et al., 2007) but has not been previously reported to be centromeric in *Drosophila* embryos or somatic cells (Lehner and O'Farrell, 1989). We analyzed CYCA localization in *Drosophila* cells and found that, in addition to its broader cellular distribution, CYCA is enriched at centromeres in both interphase and mitosis (Fig. 1 B and Fig. S3, A and B). Costaining with antibodies to CYCA and different cell cycle markers (not depicted) and time-lapse analysis of CYCA-GFP (Video 4) demonstrated that centromere enrichment increased significantly after entry into mitosis and decreased after entry into anaphase, which is coincident with the general degradation of CYCA (Lehner and O'Farrell, 1989). GFP-RCA1 displayed no obvious concentration at centromeres or chromatin and instead was distributed throughout the nucleus in early M phase, disappeared as M phase continued, and reappeared early in G1 (Fig. 1 B, Fig. S3 A, and Video 5) in a manner similar to that reported in cycle 16 *Drosophila* embryos (Grosskortenhaus and Sprenger, 2002).

Published December 1, 2008

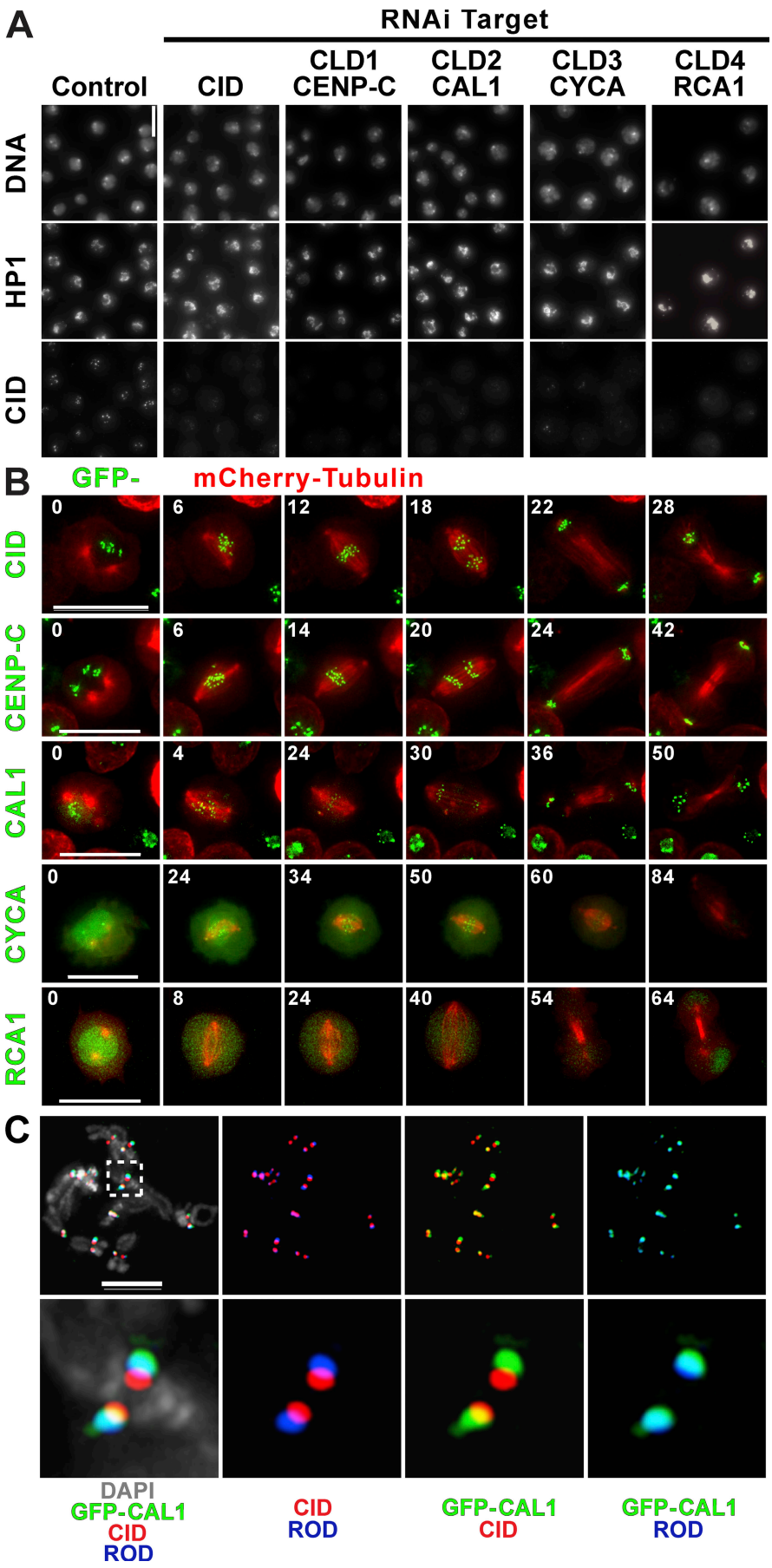

Figure 1. **Identification and localization of CLDs.** (A) IF of cells depleted of the top four positive hits from the screen. Cells were stained for DNA, CID, and HP1. CID localization to the centromere (bottom) is highly reduced or absent after RNAi depletion of all four candidates or CID in comparison with the control (left), and HP1 staining is normal in all cases. Notice that in addition to CID depletion, RCA1 and CYCA RNAi result in endoreduplication and an increase in nuclear size. (B) CLD dynamics through mitosis. Still images from time-lapse analysis of stable S2 cell lines expressing mCherry-tubulin (red) and GFP-CID, –CENP-C, -CAL1, -CYCA, and -RCA1; relative times in minutes from the start of the video are indicated in each frame. See Videos 1–5 (available at http://www.jcb.org/cgi/content/full/jcb.200806038/DC1). (C) Localization of GFP-CAL1, CID, and Rod. Metaphase chromosome spreads of S2 cells stably expressing GFP-CAL1 were stained with anti-CID (red), anti-GFP (green), and anti-Rod (blue) antibodies. The GFP-CAL1 signal overlapped significantly with the outer kinetochore protein Rod, whereas only a little overlap was observed with CID, indicating that CAL1 is located close to the outer kinetochore in mitotic chromosomes, which is in contrast to localization to CID chromatin in interphase. Inset shows magnification of image. Bars: (A) 15 μm; (B and C) 5 μm.

Published December 1, 2008

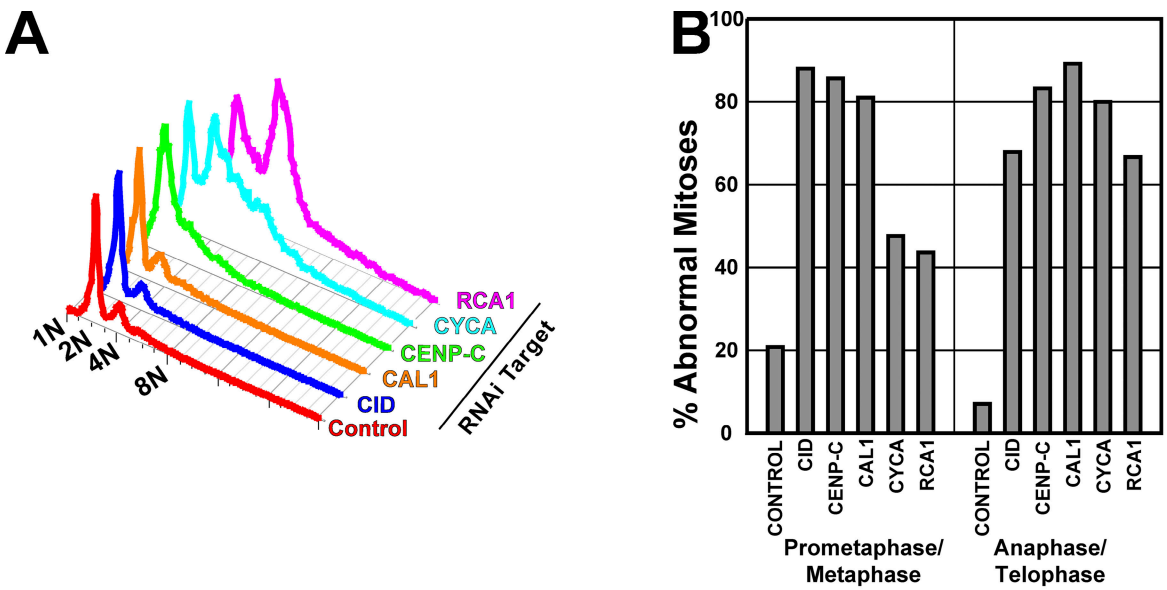

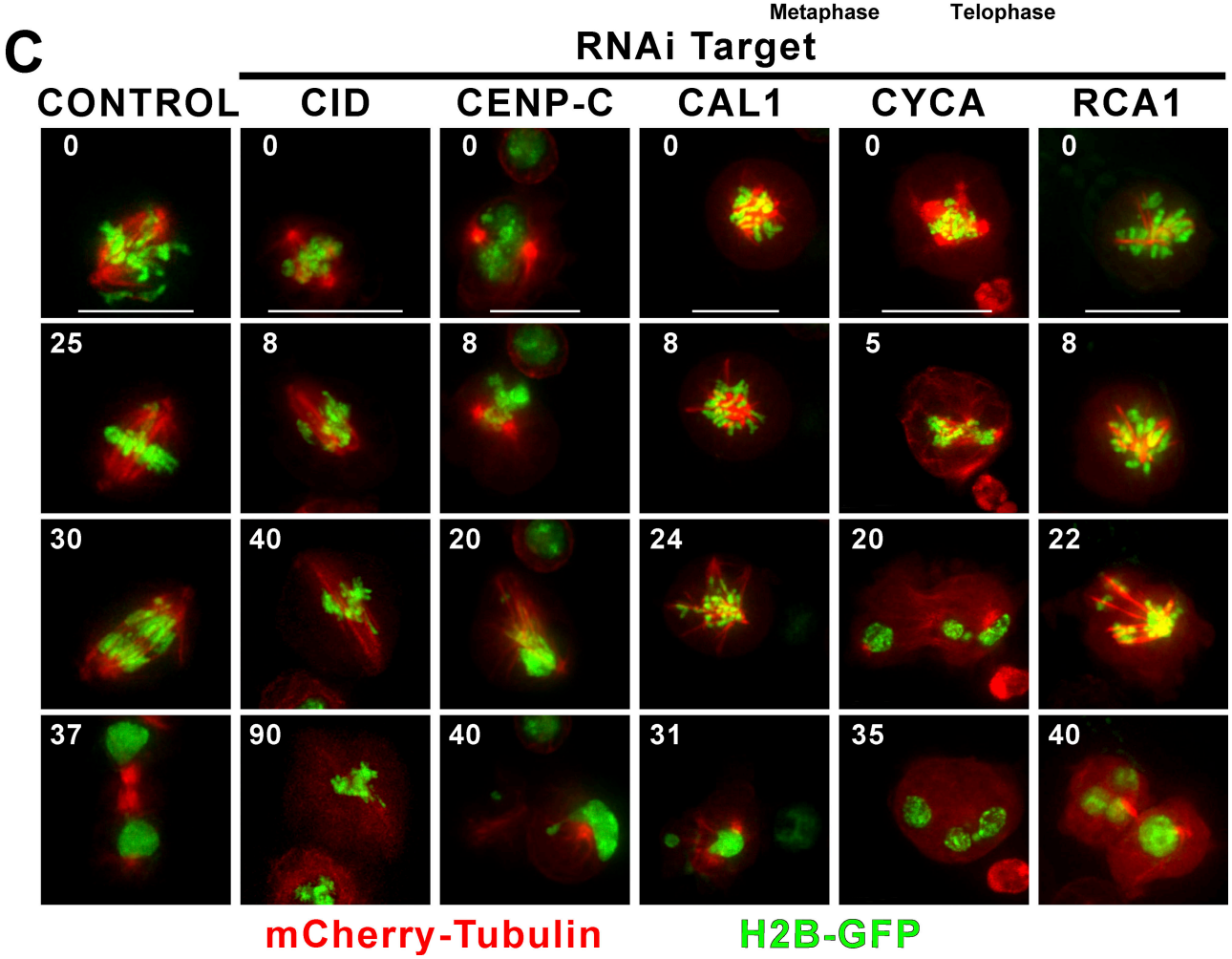

Figure 2. **Mitotic defects caused by CLD depletion.** (A) FACS analysis of control and CLD-depleted Kc167 cells. The graph shows the distribution of the DNA content of control and dsRNA-treated cells after a 4-d incubation with dsRNA. Ploidy is shown on the x axis. A high number of polyploid cells accumulated after CYCA and RCA1 depletion. A milder effect on ploidy was observed in CENP-C–depleted cells. (B) The number of defective mitoses was quantified after a 4-d incubation with control (no RNA; $n = 38$), CID ($n = 53$), CENP-C ($n = 50$), CAL1 ($n = 58$), CYCA ($n = 31$), or RCA1 ($n = 34$) dsRNA. n represents the number of cells examined in each condition. The percentage of cells with abnormal prometaphase or metaphase figures is shown on the left, and the percentage of cells with abnormal anaphase or telophase figures is shown on the right. The data are taken from a single experiment, but a duplicate experiment yielded similar results. (C) Still frames from time-lapse experiments of mitotic defects associated with RNAi depletion of CLDs in cells expressing mCherry-tubulin and H2B-GFP. Control cells (left) displayed accurate and timely chromosome segregation. CID-, CENP-C–, and CAL1-depleted cells showed a dramatic mitotic delay, little to no chromosome movement, abnormally elongated and defective spindles, and chromosome

Published December 1, 2008

GFP-CAL1 colocalized with CID at centromeres in interphase cells, which is consistent with previous localization data (Goshima et al., 2007), and also displayed diffuse staining associated with the nucleolus, around which *Drosophila* centromeres typically cluster (Fig. 1 B and Fig. S3, A and C). In metaphase cells, GFP-CAL1 associated with centromeres and also displayed weak staining throughout the nucleus. Colocalization with the outer kinetochore protein rough deal (Rod; Scaerou et al., 1999) suggested that GFP-CAL1 is associated with the outer kinetochore in mitotic chromosomes (Fig. 1 C). However, GFP-CAL1 colocalizes with CID in interphase when there is no outer kinetochore. In time-lapse experiments (Video 3), GFP-CAL1 was highly concentrated at centromeres during interphase and prophase, became less prominent at centromeres at metaphase, and then increased again starting in late anaphase. These results indicate that CAL1 is a constitutive CENP with unique centromere and kinetochore localization dynamics.

CLD protein depletion results in chromosome segregation defects

Defects in centromere and kinetochore assembly cause chromosome missegregation, mitotic delays, and defects in mitotic spindle assembly. FACS analysis showed little change in DNA content after CID and CAL1 RNAi as compared with control cells (Fig. 2 A), although CAL1 depletion caused a fourfold increase in the mitotic index (control = 0.9 ± 1.7% of mitotic cells and CAL1 RNAi = 3.7 ± 1.6% of mitotic cells; error = SD; $P < 0.005$). In contrast, depletion of CENP-C, CYCA, or RCA1 caused a significant increase in cell ploidy. CYCA- and RCA1-depleted cells showed progressive accumulation of polyploid cells by FACS analysis resulting in a >4N DNA content (Fig. 2 A) and a large increase in nuclear size in 85% of CYCA and 88% of RCA1 cells compared with 1% of control cells. These changes in DNA content and nuclear size are consistent with endoreduplication of DNA without intervening cell division previously reported for CYCA- and RCA1/Emi1-depleted *Drosophila* and human cells (Mihaylov et al., 2002; Machida and Dutta, 2007).

Analysis of fixed cells after depletion of CID, CAL1, or CENP-C demonstrated that >80% of mitoses had defects in prometaphase and metaphase chromosome alignment, and >60% of cells showed defective anaphases and telophases with missegregated or lagging anaphase chromosomes ($P < 0.01$ compared with controls; Fig. 2 B). 2.7% of CYCA- and 1.8% of RCA1-depleted cells entered mitosis, of which 80% and 66%, respectively, had abnormal anaphases and telophases with missegregated and lagging chromosomes ($P < 0.01$ compared with controls). The defects in prometaphase and metaphase stages after CYCA and RCA1 depletion were not significantly different from controls.

Time-lapse analysis of untreated S2 cells stably expressing mCherry-tubulin and histone H2B-GFP showed normal progression through mitosis (Fig. 2 C, control; and Video 6, available at http://www.jcb.org/cgi/content/full/jcb.200806038/DC1). Consistent with previous observations, CID-depleted cells were delayed in mitosis with defective spindles, abnormal chromosome condensation, and severe chromosome segregation defects (Fig. 2 C and Video 7; Blower and Karpen, 2001; Blower et al., 2006; Heun et al., 2006). CENP-C and CAL1 were identified recently in a mitotic defects screen in *Drosophila* S2 cells (Goshima et al., 2007), and our time-lapse analysis showed that CENP-C or CAL1 depletion resulted in defective spindles and chromosome condensation, little or no chromosome movement, and unequal chromosome segregation (Fig. 2 C and Videos 8 and 9). The CYCA- (Fig. 2 C and Video 10) and RCA1-depleted (Fig. 2 C) cells that entered mitosis displayed defective spindles, defective chromosome segregation, a mitotic delay with condensed chromosomes, and failed cytokinesis resulting in multinucleate cells (control = 0.9%, CYCA = 4.5%, and RCA1 = 5% multinucleate cells; Fig. 2 C). The mitotic defects we observe after CYCA and RCA1 depletion are likely to be the result of both the loss of centromere function and deregulation of the cell cycle caused by the loss of CYCA-dependent kinase activity.

Genetic and physical interactions among CLDs

We examined the interdependence between CLDs for centromere targeting by depleting each gene and localizing the other CLD proteins. Consistent with the results from our screen, epistasis analysis showed that CID is dependent on all the CLDs for its localization (Figs. 1 A and 3 A). The depletion of CID, CAL1, CYCA, or RCA1 all resulted in the loss of CENP-C from centromeres (Fig. 3 A). In addition, CAL1 depletion caused diffuse localization of CENP-C throughout the nucleus, suggesting a delocalization of CENP-C from the centromere rather than loss of CENP-C protein. CID, CENP-C, CYCA, or RCA1 depletion resulted in significant loss of CAL1 from centromeres, although CENP-C depletion produced residual, diffuse CAL1 staining, suggesting delocalization and not the loss of CAL1 (Fig. 3 B). The impact of CYCA and RCA1 depletion was weaker than observed for CID and CENP-C depletion (Fig. 3 B). CYCA enrichment at interphase centromeres was lost after CID, CENP-C, or CAL1 RNAi, and depletion of RCA1 resulted in a general decrease in CYCA staining (Fig. 3 C). Similar relationships were observed when we examined centromere localization dependencies in mutant embryos (Fig. S4 A, available at http://www.jcb.org/cgi/content/full/jcb.200806038/DC1), demonstrating the importance of these factors for centromere localization in animals. We conclude that the centromere localizations of CID, CAL1, CENP-C, and CYCA exhibit significant interdependence (Fig. 3 E).

Previous studies in human cells demonstrated that CENP-A and CENP-C coimmunoprecipitate, although a direct interaction has not been demonstrated (Ando et al., 2002; Foltz et al., 2006).

missegregation; nevertheless, cytokinesis occurred. CYCA depletion caused defective spindles, missegregation of chromosomes, and cytokinesis defects. RCA1 depletion predominantly caused a cell cycle arrest; most cells did not divide after RNAi treatment. Times are minutes from the start of the video (see Videos 6 [control], 7 [CID-RNAi], 8 [CENP-C–RNAi], 9 [CAL1-RNAi], and 10 [CYCA-RNAi], available at http://www.jcb.org/cgi/content/full/jcb.200806038/DC1). Bars, 5 µm.

Published December 1, 2008

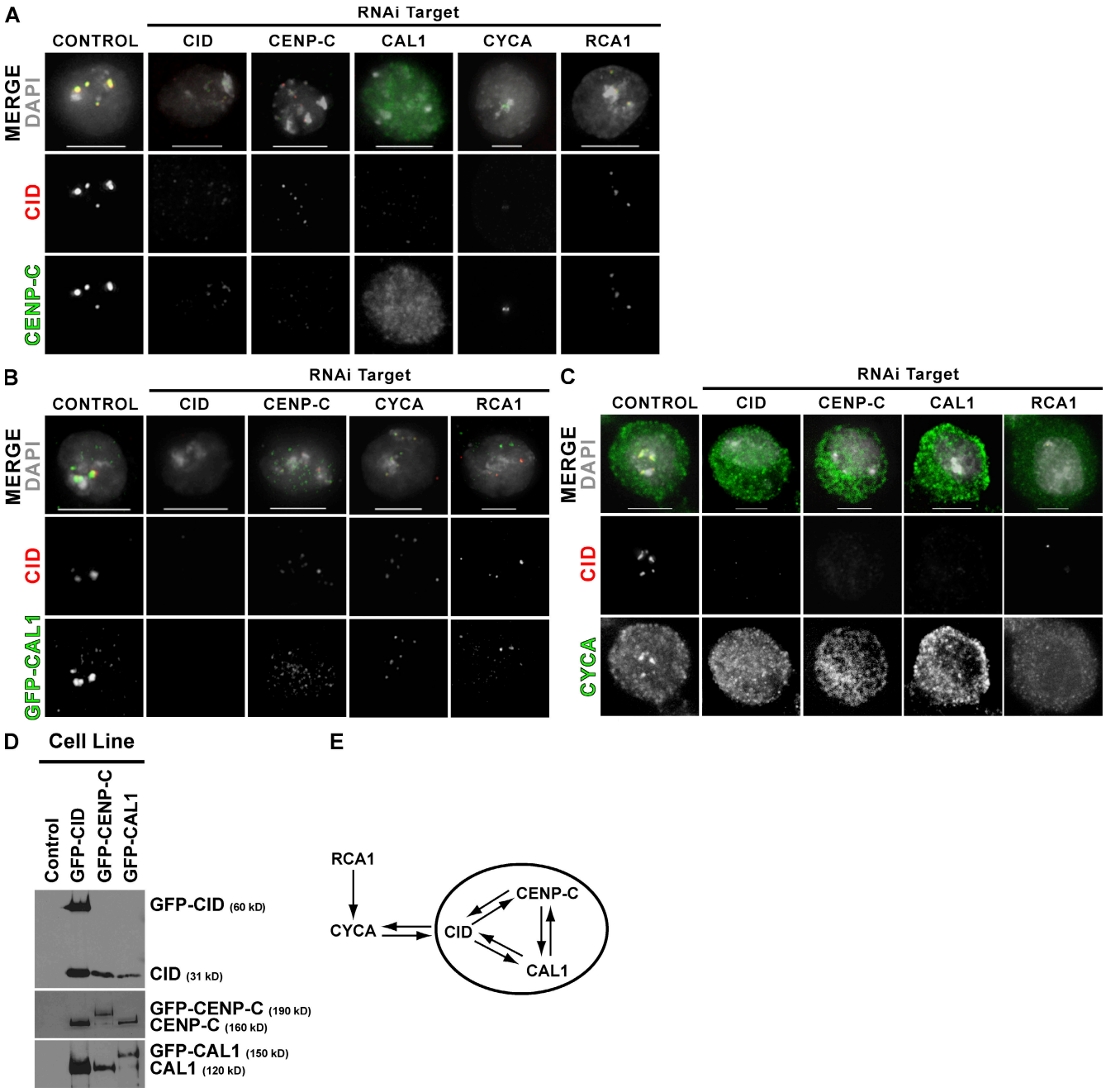

Figure 3. **CLDs are interdependent for centromeric localization and are physically associated.** (A) CLD depletions cause CID and CENP-C mislocalization. Control cells showed strong centromeric localization of CID (red) and CENP-C (green; merged panel across top; DAPI shown in gray). Depletion of CID, CENP-C, CAL1, CYCA, and RCA1 all resulted in absent or reduced centromeric staining of CID and CENP-C. Note that CAL1 depletion resulted in diffuse mislocalization of CENP-C in the nucleus, which is in contrast to the elimination of CENP-C observed after CID depletion. In addition, residual centromeric CID staining was observed after CENP-C depletion. (B) CID or CLD depletion causes loss of centromeric CAL1. Control cells showed strong colocalization between CID (red) and GFP-CAL1 (green), whereas cells depleted for CID, CENP-C, CYCA, or RCA1 displayed severely reduced centromeric CAL1. (C) Centromeric enrichment of CYCA (green) was visible in control cells and was lost in cells depleted for CID (red) after CID, CENP-C, or CAL1 RNAi (DNA is shown in gray). RCA1 depletion resulted in a general decrease in CYCA staining. (D) Coimmunoprecipitation of CLDs. GFP-CLD fusions were immunoprecipitated from stable cell lines expressing GFP-CID, GFP–CENP-C, or GFP-CAL1 or from the parent Kc167 cell line (control). Immunoprecipitates were Western blotted with antibodies against CID (top), CENP-C (middle), and CAL1 (bottom). The position of the GFP fusion and the endogenous protein is labeled on the right. (E) Summary of epistatic and physical relationships. CID, CAL1, and CENP-C physically interact and are interdependent for centromere localization. CID, CAL1, and CENP-C require RCA1 and CYCA for centromere localization, and CYCA requires all three for centromere enrichment. Bars, 5 µm.

We examined the physical interactions between CID and CLDs by digesting chromatin from cell lines expressing GFP-CID or GFP-CLDs to primarily mono- and dinucleosomes with micrococcal nuclease (Fig. S4 B), immunoprecipitating the GFP fusion proteins, and Western blotting with CID, CENP-C, CAL1, and CYCA antibodies (Fig. 3 D). We observed reciprocal coimmunoprecipitation of CID, CENP-C, and CAL1, suggesting that they are present in one or more complexes; however, we did

Published December 1, 2008

not detect association of CYCA with any of the immunoprecipitated proteins (unpublished data). The stable cell lines express the GFP-CLD fusions at or below the level of the endogenous protein, indicating that detecting the interactions between these proteins is not the result of overexpression (Fig. S4 C). A previous study suggested that CID exists as half octamers or "hemisomes" consisting of one copy each of CID, H4, H2A, and H2B (Dalal et al., 2007). However, our copurification of equal amounts of tagged and untagged CID from cells expressing lower amounts of tagged CID than endogenous CID is consistent with a *Drosophila* centromeric nucleosome containing more than one molecule of CID. We conclude that the interdependency of CID, CENP-C, and CAL1 centromere localization reflects the physical association of these proteins. At this time, it is unclear whether the interactions are direct and whether these proteins are present in one or more complexes.

CAL1 and CENP-C regulation of CID deposition

We analyzed the effects of CAL1 and CENP-C depletion on localization of newly synthesized CID to delineate roles for CAL1 and CENP-C in CID assembly versus maintenance. Newly synthesized CID was distinguished from preexisting CID by fusing CID to a modified O^6-alkylguanine-DNA alkyltransferase also known as the SNAP tag, which selectively reacts with O^6-benzylguanine derivatives. This tagging method has previously been used to monitor new CENP-A assembly in human cells (Jansen et al., 2007). We depleted CAL1 and CENP-C from Kc167 cells expressing SNAP-tagged CID and blocked preexisting SNAP-tagged CID in these cells with bromothenylpteridine (BTP). We then allowed time for the new synthesis of CID in the absence of CAL1 or CENP-C followed by labeling of SNAP-CID with a red fluorescent O^6-benzylguanine derivative (tetramethyl rhodamine* [TMR*]). We observed that CENP-C or CAL1 depletion prevented the centromere localization of newly synthesized CID (Fig. 4). We conclude that CENP-C and CAL1 are required for centromeric deposition of newly synthesized CID. Currently, we cannot rule out an additional role for CENP-C and CAL1 in the maintenance of CID in centromeric chromatin.

Centromere defects after CYCA or RCA1 depletion do not result from overreplication

A surprising result of our analysis was the requirement for CYCA and RCA1 in centromeric localization of CID, CENP-C, and CAL1. In metazoan cells, mitotic Cdk activity prevents rereplication by inhibiting the assembly of prereplication complexes (Arias and Walter, 2007). APC-dependent proteolysis of mitotic cyclins and geminin allow prereplication complex assembly in anaphase followed by a single round of replication in S phase. A central role for both CYCA and RCA1 in cell cycle control is to inhibit the activity of the APC. CYCA in complex with either Cdk1 or Cdk2 (CYCA–Cdk) directly phosphorylates and inactivates the APC activator FZR/CDH1, and RCA1 binds to FZR and prevents the interaction of $APC^{FZR/CDH1}$ with APC substrates (Zachariae et al., 1998; Jaspersen et al., 1999; Lukas et al., 1999; Grosskortenhaus and Sprenger, 2002). In the absence of CYCA or RCA1/Emi1, cells overreplicate their genomes because mitotic Cdk activity and geminin fail to accumulate, resulting in aberrant relicensing and reinitiation of replication origins (Arias and Walter, 2007; Machida and Dutta, 2007).

The recent observation that human CENP-A assembly occurs in late mitosis/G1 (Jansen et al., 2007) raised the possibility that the loss of CID, CAL1, and CENP-C after CYCA or RCA1 depletion could result indirectly from their effects on cell cycle progression and replication. RNAi depletion of geminin causes endoreduplication without affecting CYCA levels (Mihaylov et al., 2002). After depletion of geminin from cultured *Drosophila* cells, CID and CENP-C localization to centromeres was unperturbed (Fig. 5 A). Furthermore, in normally occurring endoreduplicated embryonic nuclei and highly polytenized salivary gland cells (not depicted), we observed CID localization to centromeres (Fig. 5 B). We conclude that mislocalization of CID, CENP-C, and CAL1 after CYCA or RCA1 depletion is not caused by the dilution of CID at centromeres after endoreplication.

$APC^{FZR/CDH1}$ activity regulates centromere assembly

RCA1 and CYCA–Cdk1 both function to inhibit the activities of the APC. We investigated the roles of RCA1, CYCA, and the APC in centromere assembly in more detail by determining whether the APC activators FZR/CDH1 and FZY/CDC20 affected CID, CAL1, and CENP-C centromere localization or nuclear protein levels. RCA1 or CYCA depletion resulted in CID and CENP-C mislocalization (Fig. 6, A and B) as well as a significant reduction in CID protein levels in nuclear extracts, although RCA1 depletion had a stronger effect than CYCA depletion on CID protein levels (Fig. 6 C). RNAi depletion of FZY or FZR alone did not reduce CID or CENP-C localization or levels (Fig. S5 A, available at http://www.jcb.org/cgi/content/full/jcb.200806038/DC1). However, simultaneous depletion of CYCA and FZR or RCA1 and FZR rescued the CID and CENP-C centromere mislocalization phenotypes (Fig. 6, A and B) and restored CID protein levels (Fig. 6 C). In contrast, simultaneous depletion of FZY/CDC20 and RCA1 or CYCA had no significant effect on CID or CENP-C mislocalization (Fig. 6 B), which is consistent with previous observations that RCA1 primarily inhibits FZR/CDH1 and not FZY/CDC20 in *Drosophila* (Grosskortenhaus and Sprenger, 2002). We conclude that the APC activator FZR plays a role in the CYCA- and RCA1-dependent regulation of centromere assembly.

CYCA could control centromere propagation either through CYCA–Cdk1 phosphorylation of centromere-specific substrates or through inhibitory phosphorylation of the APC. Cells depleted for both CYCA and FZR have low CYCA levels that are equivalent to the amounts observed after RCA1 depletion (Fig. 6 C). However, these cells still display normal centromere localization of CID and CENP-C (Fig. 5 A), demonstrating that normal levels of CYCA and its associated kinase activity are not required for centromere propagation. In *Drosophila*, the primary roles for CYCA–Cdk1 kinase and RCA1 are to inhibit premature APC activation so that A- and B-type cyclin can accumulate (Dienemann and Sprenger, 2004). In the absence of either inhibitor, mitotic cyclins are prematurely destroyed (Grosskortenhaus and Sprenger, 2002; Mihaylov et al., 2002). Deletion of the first 55 amino acids

Published December 1, 2008

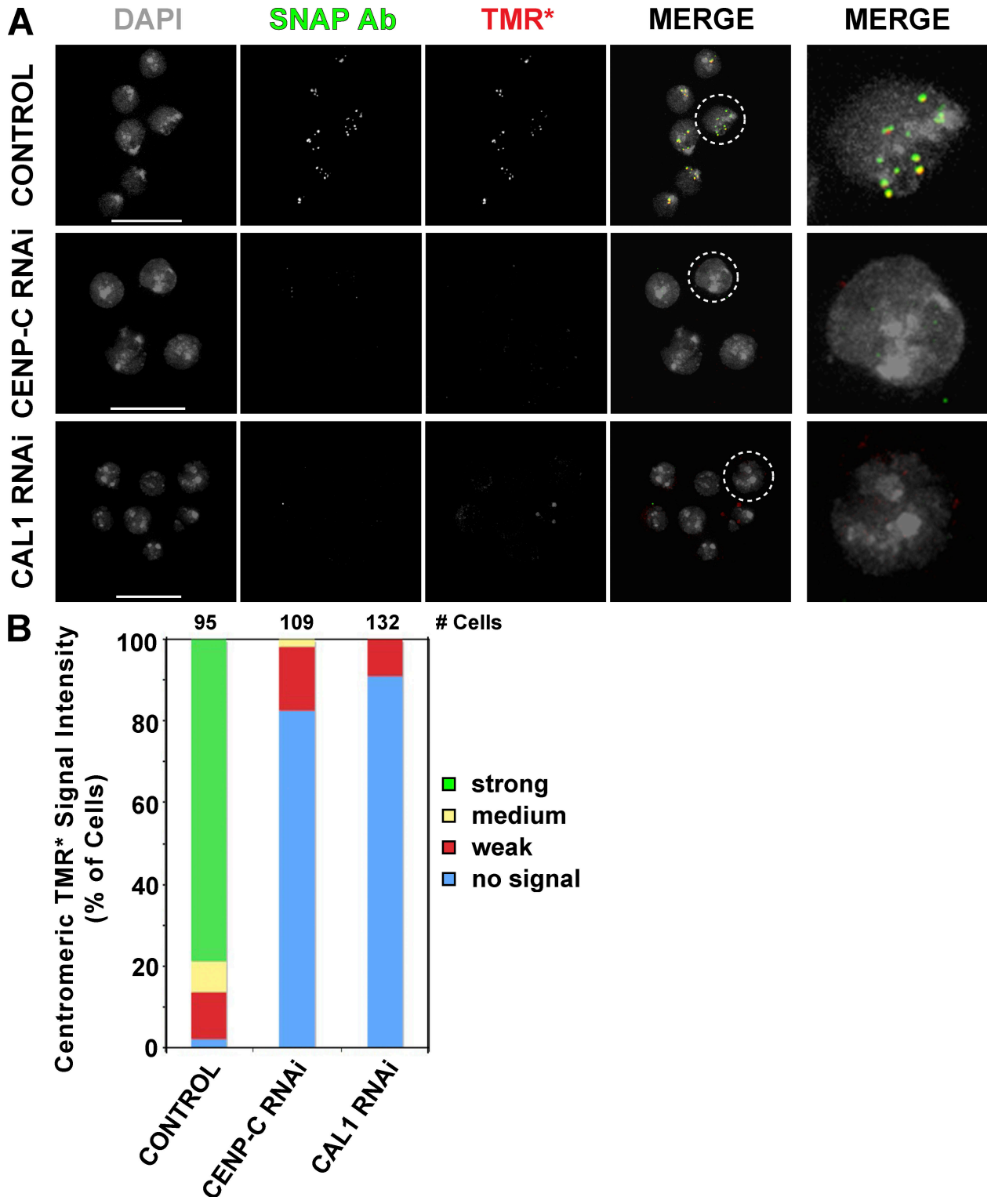

Figure 4. **CENP-C and CAL1 are required for centromeric localization of newly synthesized CID.** (A) Centromeric localization of newly synthesized SNAP-CID is defective after CENP-C or CAL1 depletion. Localization of DNA (DAPI), total SNAP-CID (SNAP Ab), and newly synthesized SNAP-CID (TMR*) are shown from representative images of cells treated with DOTAP transfection reagent only (control, top), CENP-C dsRNA (CENP-C RNAi, middle), and CAL1 dsRNA (CAL1 RNAi, bottom), respectively. Total SNAP-CID (SNAP Ab) and newly synthesized SNAP-CID (TMR*) overlap in a typical punctate centromere pattern in control cells that is not visible in CENP-C– or CAL1-depleted cells. Each image in the right panels shows an individual cell from the merge panels (dashed circle) at increased magnification. (B) Quantification of frequencies of cells with different intensities of TMR* labeling at centromeres in control cells or after CENP-C (CENP-C RNAi) or CAL1 depletion (CAL1 RNAi). Centromeric TMR* signal intensities were categorized into strong (green), medium (yellow), weak (red), or no signal (blue). The total numbers of cells used in the analysis are indicated above each graph. Most control cells display strong to medium TMR* signals at centromeres, representing normal centromere localization of newly synthesized CID. In contrast, the majority of cells contained weak or no TMR* signal after CENP-C and CAL1 RNAi, suggesting defective localization of newly synthesized CID and a role for these proteins in CID assembly. Bars, 15 μm.

Published December 1, 2008

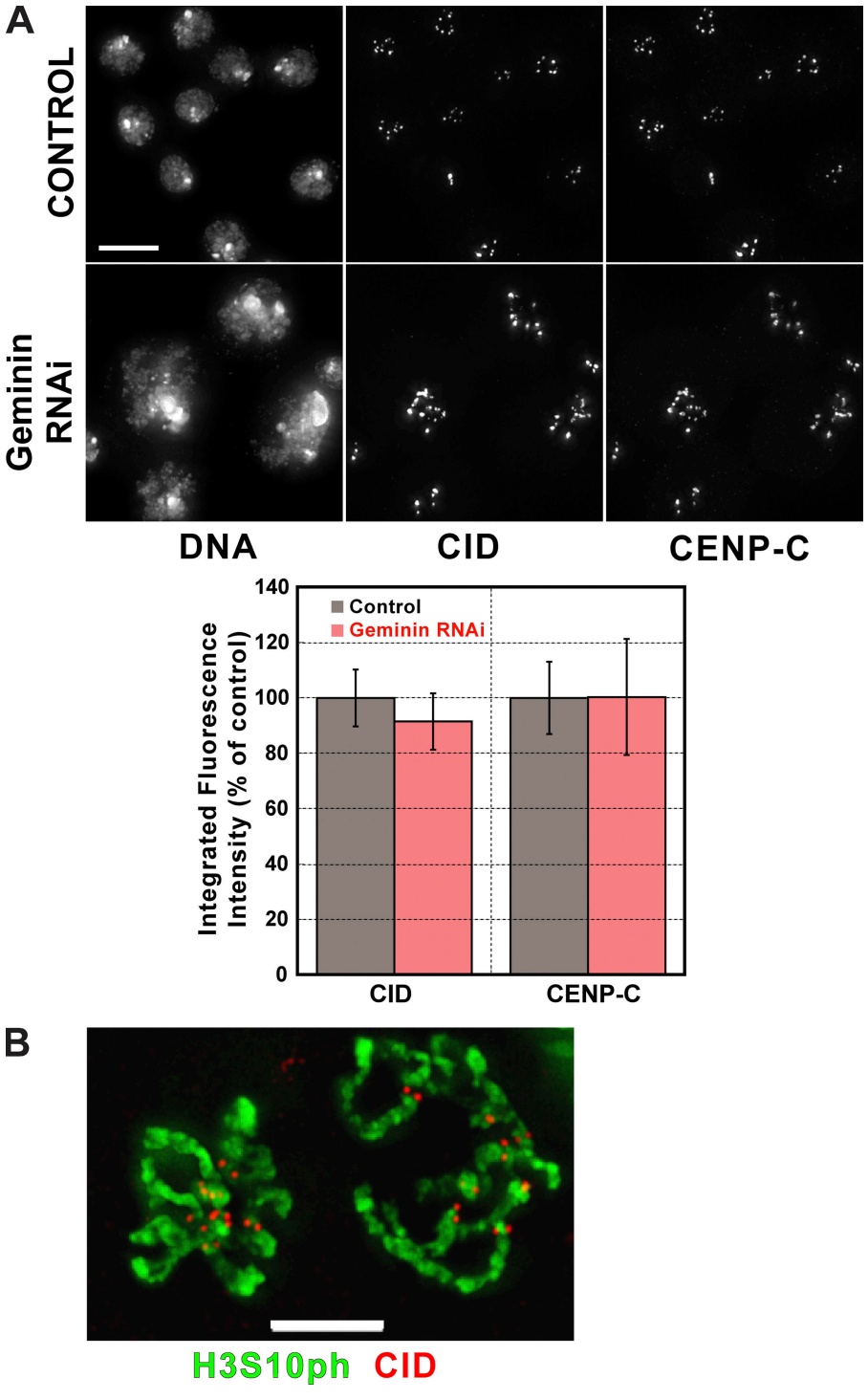

Figure 5. **Defects in centromere assembly after CYCA and RCA1 depletion do not result from overreplication.** (A) Geminin RNAi causes overreplication without loss of CID or CENP-C from centromeres. Fluorescence images of DNA, CID, and CENP-C in control cells and cells depleted of geminin. Large nuclei are indicative of overreplication in geminin-depleted cells without disruption of CID or CENP-C localization. The graph shows quantification of CID and CENP-C levels at centromeres with and without geminin depletion (n = 4; error bars represent SEM). (B) Endoreduplication naturally occurs in *Drosophila* embryos and larvae. CID (red) is present at the centromere in embryonic cells with endoreduplicated chromosomes stained for histone H3Ser10 phosphorylation (green). Bars: (A) 15 µm; (B) 5 µm.

from the amino terminus of CYCA (Δ55-CYCA) removes the destruction box and stabilizes CYCA by preventing its APC-mediated ubiquitination and destruction by the proteasome (Kaspar et al., 2001). We observed that expression of nondestructible CYCA in *Drosophila* cells depleted of RCA1 suppressed the loss of CID from centromeres (Fig. S5, C and D). Together, these observations demonstrate that proper regulation of $APC^{FZR/CDH1}$ activity is essential for controlling centromere propagation.

Previous studies showed that proteolysis facilitates formation of a single centromere by degrading noncentromeric CENP-A in yeast and flies and that CENP-A at centromeres is protected from proteolysis (Collins et al., 2004; Moreno-Moreno et al., 2006). Our results suggest that $APC^{FZR/CDH1}$ activity also controls centromere propagation by coupling centromeric chromatin assembly to the cell division cycle. In the absence of CYCA and RCA1, the premature activation of $APC^{FZR/CDH1}$ may result in the premature degradation of an APC substrate required for centromere propagation. CID levels are significantly reduced when CAL1 or RCA1 is depleted from cells (Fig. 6 C), and FZR/CDH1 RNAi rescued the reduction in

Published December 1, 2008

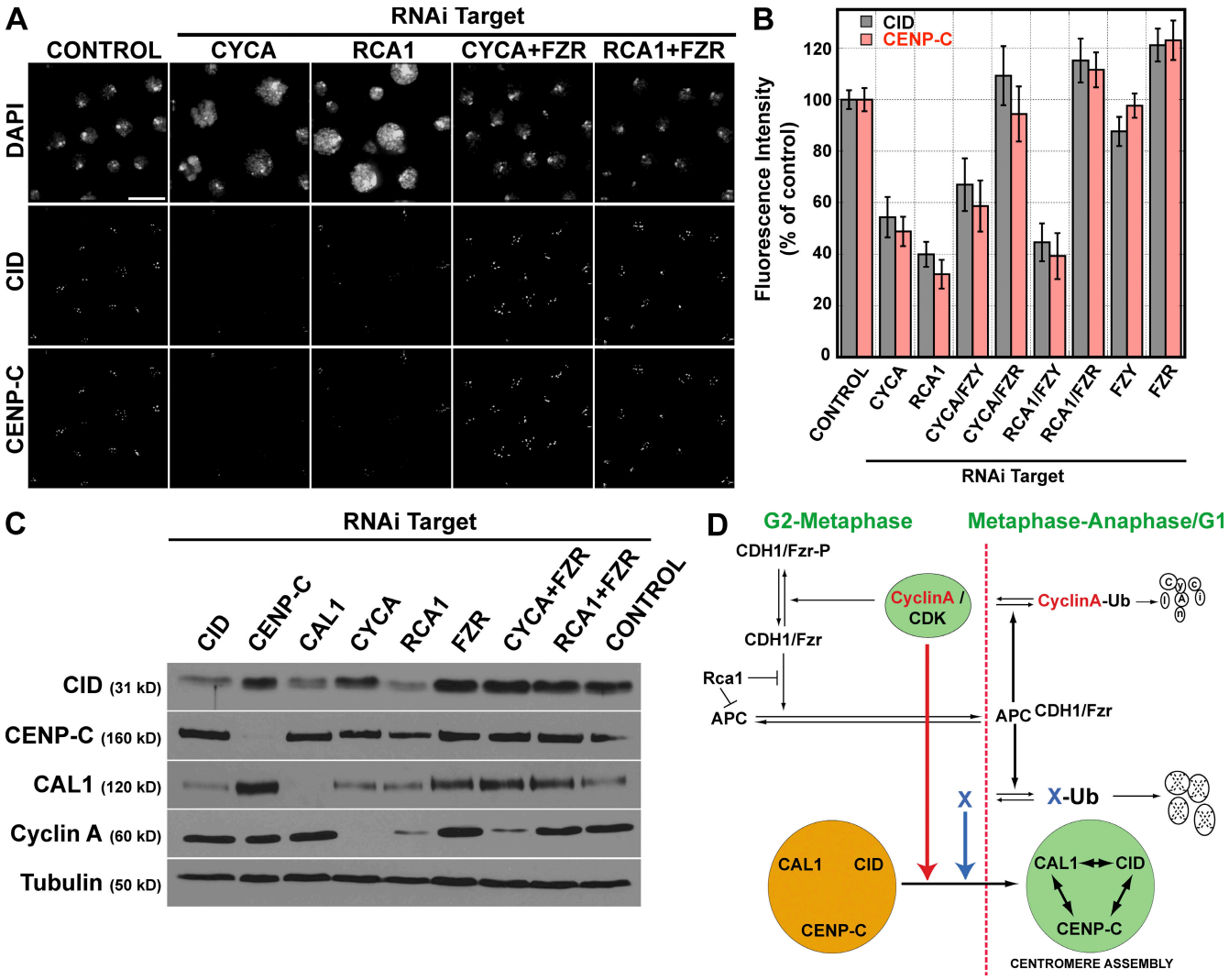

Figure 6. **Rescue of centromere assembly by APC inhibition.** (A) CYCA and RCA1 disruption of CID localization is rescued by FZR depletion. Localization of DNA (top), CID (middle), and CENP-C (bottom) in Kc167 cells treated with CYCA, RCA1, CYCA + FZR, or RCA1 + FZR dsRNAs. Control cells were not treated with dsRNA. (B) Quantification of CID and CENP-C fluorescence intensity levels at centromeres after RNAi treatment. Quantification of FZY-depleted cells is also included, showing specificity of the rescue by FZR depletion (n = 2; error bars represent SEM). (C) Protein levels of CID (31 kD), CENP-C (160 kD), CAL1 (120 kD), and CYCA (60 kD) after RNAi depletion in Kc167 cells. Nuclear extracts from Kc167 cells treated with no dsRNA (control) or dsRNA specific for CID, CENP-C, CAL1, CYCA, RCA1, FZR, CYCA + FZR, or RCA1 + FZR were Western blotted with antibodies against CLD genes or tubulin (50 kD) as a control. (D) Model for the role of CLD genes in cell cycle regulation of centromere assembly. The green background indicates proteins that localize to the centromere, orange indicates that the proteins are not competent for centromere assembly, and double arrowheads indicate that the protein or complex is required for the centromere localization of CYCA and CID-, CAL1-, and CENP-C–interdependent assembly. The APC substrate could be CYCA (red arrow) or CID, CAL1, or an unidentified substrate, X (blue arrow). Bar, 15 μm.

CID protein levels that occurred after RCA1 depletion (Fig. 6 C). CID destabilization after CAL1 depletion could not be rescued by depletion of either FZR/CDH1 or the APC subunit CDC27 (Fig. S5 A), and CID localization to centromeres in CAL1-depleted cells was not suppressed by the expression of Δ55-CYCA (Fig. S5 B). These results suggest that CID loss in CAL1-depleted cells does not result from $APC^{FZR/CDH1}$ degradation. The level of CAL1 at centromeres declines between metaphase and late anaphase, and CAL1 levels increase in the absence of FZR (Fig. 6 C). In contrast, CENP-C protein levels were not strongly affected by inhibition of CID, CAL1, CYCA, RCA1, and/or $APC^{FZR/CDH1}$ (Fig. 6 C). Our data suggest that CYCA, CID, and CAL1 are possible $APC^{FZR/CDH1}$ substrates that control the propagation of the centromere during cell division.

Discussion

We have screened for genes that regulate the centromeric localization of CENP-A/CID. This is the first example of a genome-wide RNAi screen for mislocalization of an endogenous chromosomal protein and provides the distinct advantage that the primary screen output is a direct readout of the phenotype of interest. This approach identified novel and known factors that control the assembly of centromeric chromatin and link centromere assembly and propagation to the cell cycle.

Although centromere assembly has been described as a hierarchical process directed by CENP-A, our data show that CID, CENP-C, and CAL1 are interdependent for centromere propagation, which is consistent with experiments in vertebrate

Published December 1, 2008

cells showing interdependence between the CENP-H–CENP-I complex and CENP-A (Okada et al., 2006). However, studies in *C. elegans* and vertebrates have not detected a role for CENP-C in CENP-A chromatin assembly, suggesting that CENP-C plays a more prominent role in regulating centromere propagation in flies (Oegema et al., 2001; Okada et al., 2006; Kwon et al., 2007). Collectively, these results suggest that CENPs that depend on CENP-A for their localization may "feed back" to control CENP-A assembly. Histone variants are assembled into chromatin both by histone chaperones (e.g., the histone H3.3–specific chaperone HIRA [histone regulatory A] that provides specificity to the CHD1 chromatin-remodeling ATPase) and by histone variant–specific ATPases (e.g., Swr1 that can use the general chaperone Nap1 or the specific chaperone Chz1 to assemble H2A.Z; Krogan et al., 2003; Kobor et al., 2004; Mizuguchi et al., 2004; Jin et al., 2005; Konev et al., 2007; Luk et al., 2007). CENP-C or CAL1 might facilitate centromere-specific CID localization by providing centromere specificity to a chromatin-remodeling ATPase in a manner analogous to HIRA or might direct the localization of chromatin assembly factors to the centromere. It will be interesting to determine what factors associate with CAL1 and CENP-C as a route to elucidating the mechanisms of centromere assembly and propagation.

The loading of CENP-A in human somatic cells and in *Drosophila* embryos occurs after anaphase initiation (Jansen et al., 2007; Schuh et al., 2007) when $APC^{FZR/CDH1}$ activity is high (Morgan, 2007). Ubiquitin-mediated proteolysis facilitates formation of a single centromere by degrading noncentromeric CENP-A (Collins et al., 2004; Moreno-Moreno et al., 2006), and subunits of the APC are localized to kinetochores (Jorgensen et al., 1998; Kurasawa and Todokoro, 1999; Topper et al., 2002; Acquaviva et al., 2004). Our results demonstrate that normal regulation of $APC^{FZR/CDH1}$ activity is required for centromere propagation, providing a link between centromere assembly and cell cycle regulation.

We propose two alternative models for the role of $APC^{FZR/CDH1}$ in centromere function. The first model is that CYCA is the relevant substrate of $APC^{FZR/CDH1}$ and that the kinase activity of the CYCA–Cdk1 complex is required for the localization of CID, CENP-C, and CAL1 to the centromere (Fig. 6 D, red arrow). CYCA is normally degraded as cells proceed through mitosis, suggesting that CYCA–Cdk1 would likely act during G2 or early M to phosphorylate a substrate involved in centromere assembly. The CID and CENP-C localization defect caused by CYCA depletion was rescued by the simultaneous depletion of FZR/CDH1 even though the levels of CYCA protein remained low in the double depletion. The rescue of the CID and CENP-C localization defect in cells with low CYCA protein suggests that maintaining high levels of CYCA–Cdk1 activity is not required for centromere propagation, but we cannot rule out that the residual CYCA protein in these cells is sufficient to rescue the centromeric phenotype when APC activity is compromised by FZR/CDH1 depletion.

The second model that is consistent with our observations is that one or more $APC^{FZR/CDH1}$ substrates ("X") regulate the interdependent localization of CID, CENP-C, and CAL1 to the centromere (Fig. 6 D, blue arrow). RCA1 and CYCA inhibit the APC in G2 to allow mitotic cyclin accumulation. An $APC^{FZR/CDH1}$ substrate could repress centromere assembly until anaphase/G1, when proteolysis would remove the repression in a manner analogous to replication licensing. If an $APC^{FZR/CDH1}$ substrate acted solely as a negative regulator of centromere assembly, FZR/CDH1 depletion should prevent CID assembly at centromeres, and premature $APC^{FZR/CDH1}$ activation by CYCA or RCA1 depletion might cause an increase of CID at centromeres as a result of premature assembly. We observed that neither CDH1 nor CDC20 depletion alone impacted CID, CAL1, or CENP-C assembly at centromeres or the overall levels of these proteins but that premature APC activation resulted in failed centromere assembly (Fig. 6, A and B; and Fig. S5 A).

A simple interpretation of our results is that CYCA–Cdk1 or another $APC^{FZR/CDH1}$ substrate acts during G2/metaphase before $APC^{FZR/CDH1}$ activation to make centromeres competent for assembly during anaphase and/or G1 (Fig. 6 D). Premature removal of the $APC^{FZR/CDH1}$ substrate would cause failure to relicense the centromeres for assembly in the next G1 phase. When compared with the process of replication licensing, in which the positive regulator CDC6 and the negative regulators geminin and CYCA are all substrates of $APC^{FZR/CDH1}$, the model of a single $APC^{FZR/CDH1}$ substrate that controls centromere licensing or propagation may be oversimplified. We observed that defective centromere localization of CID and CENP-C after CYCA or RCA1 depletion was not rescued by CDC20 depletion, but we cannot rule out a role for $APC^{FZY/CDC20}$ in centromere propagation because premature $APC^{FZR/CDH1}$ activation could mask a subsequent role for FZY/CDC20, which is activated at the metaphase/anaphase transition.

We do not yet know whether the localization of CYCA at centromeres is important for the regulation of centromere assembly. In *Drosophila*, it has been demonstrated that the subcellular localization of CYCA is not important for proper progression through the cell cycle; however, these experiments did not directly address whether mislocalization of CYCA prevented the association of CYCA with centromeres (Dienemann and Sprenger, 2004). It will be interesting to determine whether CID, CENP-C, and CAL1 localization require centromere-localized CYCA–Cdk1 activity or whether any of these proteins are a direct target of CYCA–Cdk1.

Our results suggest that CID or CAL1 levels are indirectly controlled by APC activity. Interestingly, the human M18BP1 has recently been proposed to act as a "licensing factor" for centromere assembly. Although no clear homologues of M18BP1/KNL2 have been identified in *Drosophila*, both CAL1 in flies and M18BP1/KNL2 in other species are interdependent with CENP-A for centromere localization (Fujita et al., 2007; Maddox et al., 2007). Strikingly, levels of CAL1 and M18BP1/KNL2 are reduced on metaphase centromeres and increase coincident with CENP-A loading in late anaphase/telophase (Jansen et al., 2007; Schuh et al., 2007). Further analysis is required to determine whether CAL1 and M18BP1/KNL2 function analogously in centromere assembly. It will be important to determine whether fly homologues of other Mis18 complex components are associated with CAL1 and important for centromere assembly. Identifying the APC substrates involved in centromere assembly will

Published December 1, 2008

be necessary to distinguish between these models and to determine how these proteins epigenetically regulate centromere assembly and couple this essential process to the cell cycle.

Materials and methods

Genome-wide RNAi screen

Logarithmically growing Kc167 cells were trypsinized, washed, and resuspended in serum-free medium at 1 × 10^6 cells/ml, and 10 µl of cells was plated to each well of the 384-well plate containing dsRNA. Cells were incubated for 1 h at room temperature before 35 µl of Schneider's medium (Invitrogen) with 1× antibiotics (Invitrogen), and 10% FCS (Omega) was added to each well and incubated for an additional 4 d at 25°C. Cells were fixed for 5 min at room temperature in 100% methanol and washed twice in 1× TBS with 0.1% Triton X-100 (TBST). Cells were treated for 30 min with blocking solution (TBST containing 2% BSA), which was replaced by 10 µl of blocking solution containing chicken anti-CID antibody (1:100 dilution) and mouse anti-HP1 (1:400 dilution) and incubated overnight at 4°C. Cells were washed twice for 5 min with blocking solution, and 10 µl of secondary antibodies (Alexa 568 anti–chicken and Alexa 488 anti–mouse antibody at 1:400 dilutions) was added and incubated for 1 h at room temperature. Secondary antibodies were washed away three times with TBST. DNA was stained with 2 µg/ml Hoechst 33342 in TBS for 10 min at room temperature and washed with TBS. Plates were imaged using a 40× objective using an automated plate-imaging microscope (ImageXpress; MDS Analytical Technologies).

A MetaMorph (available at http://straightlab.stanford.edu/analysis) journal was written to segment nuclei based on DNA staining. Cell area was estimated by a 10-pixel dilation from the nuclei. Centromere staining was identified within the cells through a morphological top hat filter with a 5-pixel diameter. The integrated intensity of the centromere and cell body staining was collected. Each well was assigned a score equal to the sum of the cell body intensity divided by the sum of the centromere intensity. Positives were verified by manual image analysis and retesting (Fig. S1).

Indirect IF on fixed cells

S2 cells were settled on glass slides and fixed with either 4% PFA, 4% formalin, or 100% methanol for 10 min. After three washes with PBS for 10 min each, cells were blocked in either 5% milk or 2% BSA in PBST (PBS with 0.2% Triton X-100) for 10 min before primary antibody incubation overnight at 4°C followed by three washes of 10 min in PBST. To detect the kinetochore localization of GFP-CAL1, a stable line expressing GFP-CAL1 was treated with 0.5% sodium citrate for 7 min followed by centrifugation on a slide using cytospin (Shandon) at 2,900 rpm for 10 min; cells were then fixed, washed, blocked in PBST with 5% milk, and incubated overnight at 4°C with anti-CID and anti-Rod antibodies. After washes and incubation with anti–chicken and anti–rabbit secondaries, cells were fixed again for 5 min with 4% formalin, washed, and incubated overnight with Alexa 488–conjugated anti-GFP antibody (Invitrogen). All of the secondary antibodies used were Alexa 488, Alexa 546, or Alexa 647 (Invitrogen) conjugates, and they were incubated at 1:500 dilutions for 45 min at room temperature. After three 10-min washes in PBS, cells were mounted in 2.5% 1,4-diazabicyclo[2.2.2]octane and 1 µg/ml DAPI in 50% glycerol. The dilutions and antibodies used were 1:300 chicken anti-CID (Blower and Karpen, 2001), 1:300 guinea pig anti–CENP-C, 1:500 rabbit anti-GFP (Invitrogen), 1:10 mouse anti-CYCA (Developmental Studies Hybridoma Bank), 1:500 mouse antitubulin (Sigma-Aldrich), 1:500 rabbit anti-PH3 (H3S10ph; Millipore), 1:500 mouse antifibrillarin (Cytoskeleton, Inc.), and 1:500 rabbit anti-Rod (Scaerou et al., 1999). All images were taken on a microscope (Deltavision Spectris; Applied Precision, LLC) and deconvolved using softWoRx (Applied Precision, LLC). Images were taken as z stacks of 0.2- or 0.3-µm increments using a 100× oil-immersion objective.

Embryos were collected either overnight or for 1 h, aged, and dechorionized with 50% bleach for 2 min. Embryos extensively washed in 100 mM NaCl + 0.5% Triton X-100 were fixed with formaldehyde saturated with heptane for 20 min and hand devitillinized on double sticky tape with a 35-gauge needle in PBTA (1% BSA + 0.2% Triton X-100 and 0.05% NaN_3 in PBS). Antibodies were diluted in PBTA and incubated overnight. After three 10-min washes in PBTA, secondary antibodies were incubated for 2 h. After three washes in PBS, embryos were mounted in Vectashield containing DAPI and imaged on a Deltavision microscope as stated in the previous paragraph. The mutant embryos used for this study were *y*, *ry* (control), *cycA*^{C8LR1}, *cenpC*$^{prl\text{-}41}$ (C. Lehner, University of Zurich, Zurich, Switzerland), *rca1*^{IX}, and *pBacCG5148*.

CENP-C antibodies were generated by cloning the first 2,196 bp of the DmCENP-C gene into the pET100/D-TOPO vector (Invitrogen). Protein was expressed in BL21-star cells and purified using the pETQIA expressionist kit (QIAGEN). Polyclonal antibodies were produced in guinea pigs by Covance, and crude serum was used for immunostaining. The first 176 amino acids of CAL1 and the first 124 amino acids of CID were fused to GST using a modified pGEX-6P vector (EMD). Fusion proteins were expressed in BL21 (DE3) pLysS cells and purified with glutathione agarose (Sigma-Aldrich). Polyclonal antibodies were produced in rabbits, and antisera were affinity purified against the antigen after removal of the GST tag with PreScission Protease (EMD).

Immunoprecipitation from Kc167 cells

Approximately 8 × 10^{10} cells stably expressing GFP-tagged CLD proteins at levels equal to or lower than the endogenous levels were harvested and washed in PBS. Nuclei were isolated by lysing the cells in 25 ml of nuclear extraction buffer (20 mM Hepes, pH 7.7, 50 mM KCl, 2 mM $MgCl_2$, 5 mM β-mercaptoethanol [β-ME], 1% Triton X-100, 1 mM PMSF, 2 mM benzamidine-HCl, and 10 µg/ml LPC [leupeptin, pepstatin, and chymostatin]) followed by a wash in 25 ml of nuclear wash buffer (20 mM Hepes, pH 7.7, 50 mM KCl, 2 mM $MgCl_2$, 5 mM β-ME, 1 mM PMSF, 2 mM benzamidine-HCl, and 10 µg/ml LPC). Nuclei were resuspended in 3 ml of micrococcal nuclease buffer (20 mM Hepes, pH 7.7, 50 mM KCl, 2 mM $MgCl_2$, 5 mM β-ME, 3 mM $CaCl_2$, 1 mM PMSF, 2 mM benzamidine-HCl, and 10 µg/ml LPC), and chromatin was digested with 0.1 U/µl micrococcal nuclease (Worthington Biochemical) for 30 min at 25°C. 3 ml of 2× extraction buffer (20 mM Hepes, pH 7.7, 575 mM KCl, 5 mM EGTA, 5 mM EDTA, 5 mM β-ME, 20% glycerol, 0.1% Igepal-CA630, 1 mM PMSF, 2 mM benzamidine-HCl, and 10 µg/ml LPC) was added to stop the reactions. The lysate was sonicated twice for 30 s and cleared by centrifugation at 10,000 *g* for 15 min. Cleared lysate was added to 30 µl of anti-GFP resin (0.5 mg/ml polyclonal rabbit anti-GFP antibody coupled to protein A–Sepharose beads) and incubated for 2 h at 4°C. The anti-GFP resin was washed three times in 20 mM Hepes, pH 7.7, 300 mM KCl, 2.5 mM EGTA, 2.5 mM EDTA, 5 mM β-ME, 10% glycerol, 0.05% Igepal, 1 mM PMSF, 2 mM benzamidine-HCl, and 10 µg/ml LPC, boiled in 70 µl of SDS sample buffer, and analyzed by Western blotting.

Western blotting

Approximately 4 × 10^7 cells were harvested and washed once in PBS. The cells were lysed in 20 mM Hepes, pH 7.7, 500 mM NaCl, 5 mM EDTA, 5 mM EGTA, 0.5% Igepal, 1 mM PMSF, 2 mM benzamidine-HCL, and 10 µg/ml LPC. Protein concentrations were equalized by Bradford assays, and 30 µg of total protein was loaded per sample. Proteins were transferred to a nitrocellulose membrane in 10 mM 3-(cyclohexylamino)-1-propane sulfonic acid, 0.1% SDS, and 20% methanol for 45 min for CID and CYCA or for 90 min for CENP-C and CAL1. Affinity-purified antibodies were used at a concentration of 1 µg/ml.

FACS analysis

Kc167 cells were grown in 6-well dishes and harvested at 24, 48, 72, and 96 h after RNAi treatment. Cells were washed once in PBS and fixed by dropwise addition into 70% ethanol while mixing. Cells were washed twice in PBS. The cells were stained by the addition of 100 µl of 100 µg/ml RNaseA and 400 µl of 50 µg/ml propidium iodide. DNA content was measured using a FACS analyzer (FACScan; BD). FACS data were analyzed with FlowJo software (Tree Star, Inc.).

RNAi depletion

dsRNA was prepared using a kit (MegaSCRIPT T7; Applied Biosystems) according to the manufacturer's procedures. Templates were generated by PCR from genomic DNA using the following primers: CYCA reverse, 5′-GCCAAGAAATCGAATGTGGT-3′; CYCA forward, 5′-ATTTCACGTCATGGTTCTCTT-3′; RCA1 reverse, 5′-TTTCAATCGCCACACAGTAG-3′; RCA1 forward, 5′-GCCTCGCTTATGAAAACCC-3′; CAL1 forward, 5′-TGGATGCCAGGAAAGTTAGT-3′; CAL1 reverse, 5′-CTATAGGGATTGTTGATATCAGC-3′; CENP-C forward, 5′-TGGTAAACTATTTGGGTCTCTC-3′; CENP-C reverse, 5′-GGTACCAGTTCGTTCTCCA-3′; CID forward, 5′-ACCGTGCAGCAGGAAAG-3′; and CID reverse, 5′-CCCCGGTCGCAGATGTA-3′. 10^6 logarithmically growing S2 cells were plated in 1 ml of serum-free medium, and 15 µg dsRNA was added to the culture. Control wells received water instead of dsRNA. After 1 h of incubation, 1.5 ml of serum-containing medium was added, and incubation proceeded for 4 d. Samples of 100 µl were taken every day and were subjected to indirect IF analysis.

Published December 1, 2008

Quantitation of defective mitoses and mitotic index
S2 cells were depleted of CID, CLD-2, CENP-C, RCA1, or CYCA by RNAi. After 4 d, cells were fixed for 10 min with 10% formalin in PBS and stained for DNA (DAPI), CID, CENP-C, tubulin, or H3S10Ph by indirect IF. Mitotic cells were scored as defective or normal based on chromosome and spindle morphology compared with control cells, and the significance of the differences was determined using the χ^2 test.

SNAP tag labeling of newly synthesized CID
Drosophila Kc cells stably expressing SNAP-tagged CID (SNAP-CID) were transfected with 5 µg dsRNA against CENP-C or CAL1 using the 1,2-dioleoyl-3-trimethylammonium-propane (DOTAP) transfection reagent (Roche) or transfection reagent alone (control). SNAP-CID was quenched with BTP after 72 h of RNAi depletion. BTP was removed, and cells were allowed to grow for another 24 h to allow synthesis of unlabeled SNAP-CID protein followed by TMR* labeling. Cells were fixed with 4% formaldehyde in PBST for 5 min, and total SNAP-CID was detected by IF with a rabbit α-SNAP polyclonal antibody (Covalys) used at 1:500.

Time-lapse analysis and GFP constructs
Time-lapse videos were performed using a Deltavision Spectris microscope. Cells were mounted using the hanging drop method (Heun et al., 2006). For the mitotic time-lapse videos, cells expressing mCherry-tubulin and H2B-GFP in prophase/prometaphase (gift of G. Goshima and R. Vale, University of California, San Francisco, San Francisco, CA) were imaged every 1 or 2 min until cytokinesis for a total of 30–45 min with the exception of CID RNAi, in which, in some severe cases, cells were imaged for 90–120 min and did not undergo cytokinesis. Cells were imaged 3–4 d after RNAi treatment except for CYCA and RCA1 RNAi, in which cells were imaged after 1–2 d of treatment. 5–10 videos of randomly selected prophase cells were imaged for each RNAi experiment. 80–100% of videos per RNAi experiment showed mitotic defects with the exception of CYCA and RCA1 RNAi, in which the percentage of defective mitoses was ∼60%. Videos of GFP-CID, GFP-CDL2, GFP–CENP-C, and GFP-CYCA in mCherry-tubulin–expressing cells were imaged every 2 min until cytokinesis was completed. Videos were edited in Photoshop (Adobe) to reduce video size, and the time in minutes in the still images reflects the actual elapsed time during image acquisition.

GFP constructs were generated for all five CLD genes after PCR amplification with a template PCR system (Expand Long; Roche) from either *Drosophila* Genomic Resource Center clones or from *Drosophila* Kc167 cell poly-A RNA using the following primers flanked by an AscI site at the 5′ end and a PacI site at the 3′ end: CID forward, 5′-GCATCATATGCAGCACGCTGTTTCCGCTG-3′; CID reverse, 5′-GCATGCTAGCGCTTTTTTGGAACAGTGTGACCG-3′; CG5148 forward, 5′-ATGGCGAATGCGGTGGTG-3′; CG5148 reverse, 5′-TTACTTGTCACCGGAATTATTCTCG-3′; CENP-C forward, 5′-ATGTCGAAGCCCCAGAAC-3′; CENP-C reverse, 5′-CTAACTGCGTATACACATCAG-3′; RCA1 forward, 5′-ATGAGCGCCTATTATCGGCG-3′; RCA1 reverse, 5′-CTAAAAGCAGAGCCGCTTGAGCGAGTT-3′; CYCA forward, 5′-ATGGCCAGTTTCCAGATCCAC-3′; CYCA reverse, 5′-ATGTCCGTGACGGATGTTCAGTC-3′; and Δ55-CYCA forward, 5′-AACAATGTGCCGCGTCCG-3′. PCR products were cloned into pCopia–localization and purification (LAP) digested with AscI and PacI. pCopia-LAP was generated by replacing EGFP with the LAP tag (Cheeseman and Desai, 2005) and modifying the polylinker such that AscI/PacI cloning would result in the N-terminal LAP (GFP) tagging of genes. The Copia promoter was PCR amplified from the pCoPuro plasmid (Iwaki et al., 2003) with the primers forward (5′-GCATCATATGGGCAAATGGGTTTAGGATTGGG-3′) and reverse (5′-GCATGCTAGCGGAAGGTCGTCTCCTTGTGAGG-3′) and was cloned into the EGFP vector using the NdeI and NheI sites. The plasmid for nondegradable cyclin expression was generated by ligating Δ55-CYCA into the AscI and PacI sites of pCopia-LAP to generate pCopia-GFP–Δ55-CYCA.

S2 cells were transfected with Cellfectin (Invitrogen) according to the manufacturer's instructions. Stable lines were obtained by cotransfecting the LAP tag constructs with the plasmid pHygro (Invitrogen) and by selection in the presence of 100 µg/ml hygromycin B (Invitrogen).

Nondegradable CYCA rescue experiments
Kc167 cells were depleted of CYCA and RCA1 by treatment with dsRNA. Immediately after the incubation of cells with dsRNA, the cells were transfected with plasmids expressing GFP, pCopia–GFP-CYCA, or pCopia-GFP–Δ55-CYCA with FuGene 6 (Roche) according to the manufacturer's instructions. After 4 d, the cells were fixed for IF and stained for DNA, GFP, and CID. CID centromere intensities were measured in the GFP-positive and GFP-negative populations.

For the experiments to test nondegradable CYCA rescue of CAL1 depletion, cells were transfected with 5 µg pCopia-GFP–Δ55-CYCA alone or in combination with 5 µg dsRNAi against CAL1 using the DOTAP transfection reagent. 4 d after incubation, cells were fixed and stained with anti-GFP and anti-CID antibodies.

Online supplemental material
Fig. S1 depicts the workflow of the genome-wide siRNA screen for centromere propagation and the quantification of CID levels after RNAi depletion of the CLD genes. Fig. S2 shows the alignment of CAL1 homologues in several drosophilid species. Fig. S3 shows the localization of CLDs in interphase and mitosis. Fig. S4 shows the effect of *cenpC*, *cal1*, *cycA*, and *rca1* mutants on centromeres in *Drosophila* embryos, the fragmentation of chromatin used in the LAP-CLD purifications, and the expression levels of LAP-CLD fusions in Kc167 cells. Fig. S5 shows the rescue of centromeric CID localization in RCA1-depleted cells by nondegradable CYCA. Videos 1–5 show time-lapse videos of *Drosophila* S2 cells expressing mCherry-tubulin and GFP-CID, GFP–CENP-C, GFP-CAL1, GFP-CYCA, and GFP-RCA1, respectively. Videos 6–10 show time-lapse videos of *Drosophila* S2 cells expressing GFP-H2B and mCherry-tubulin after dsRNA depletion with control, CID, CENP-C, CAL1, and CYCA RNA, respectively. Online supplemental material is available at http://www.jcb.org/cgi/content/full/jcb.200806038/DC1.

We thank Alison Farrell and Abby Dernburg for critical reading of the manuscript and Michael Rape for helpful discussions. We are grateful to Pat Brown, Yoav Soen, and Bob Marinelli for assistance with high throughput imaging. We are also grateful to Norbert Perrimon, Nadire Ramadan, and Bernard Mathey-Prevot (*Drosophila* RNA Interference Screening Center, Harvard, Cambridge, MA) for assistance with dsRNA screening, Gohta Goshima for reagents, Christian Lehner for *cenpC* mutant flies, and the Developmental Studies Hybridoma Bank for CYCA antibodies developed by Christian Lehner. We also thank Aki Minoda and David Seo for general technical help and the Straight and Karpen laboratories for discussion and support.

This work was supported by National Institutes of Health grants to G.H. Karpen and A.F. Straight (R01 GM066272 and R01 GM074728, respectively), grants from the Wellcome Trust to S. Erhardt, grants from Philip Morris USA, Inc. and Philip Morris International to B.G. Mellone, and grants from the Susan G. Komen Breast Cancer Foundation to W. Zhang. A.F. Straight is a Gordon Family Scholar supported by the Damon Runyon Cancer Research Foundation.

Submitted: 5 June 2008
Accepted: 30 October 2008

References

Acquaviva, C., F. Herzog, C. Kraft, and J. Pines. 2004. The anaphase promoting complex/cyclosome is recruited to centromeres by the spindle assembly checkpoint. *Nat. Cell Biol.* 6:892–898.

Ando, S., H. Yang, N. Nozaki, T. Okazaki, and K. Yoda. 2002. CENP-A, -B, and -C chromatin complex that contains the I-type alpha-satellite array constitutes the prekinetochore in HeLa cells. *Mol. Cell. Biol.* 22:2229–2241.

Arias, E.E., and J.C. Walter. 2007. Strength in numbers: preventing rereplication via multiple mechanisms in eukaryotic cells. *Genes Dev.* 21:497–518.

Bentley, A.M., G. Normand, J. Hoyt, and R.W. King. 2007. Distinct sequence elements of cyclin B1 promote localization to chromatin, centrosomes, and kinetochores during mitosis. *Mol. Biol. Cell.* 18:4847–4858.

Blower, M.D., and G.H. Karpen. 2001. The role of *Drosophila* CID in kinetochore formation, cell-cycle progression and heterochromatin interactions. *Nat. Cell Biol.* 3:730–739.

Blower, M.D., T. Daigle, T. Kaufman, and G.H. Karpen. 2006. *Drosophila* CENP-A mutations cause a BubR1-dependent early mitotic delay without normal localization of kinetochore components. *PLoS Genet.* 2:e110.

Carroll, C.W., and A.F. Straight. 2006. Centromere formation: from epigenetics to self-assembly. *Trends Cell Biol.* 16:70–78.

Cheeseman, I.M., and A. Desai. 2005. A combined approach for the localization and tandem affinity purification of protein complexes from metazoans. *Sci. STKE.* doi:10.1126/stke.2662005p11.

Clark, A.G., M.B. Eisen, D.R. Smith, C.M. Bergman, B. Oliver, T.A. Markow, T.C. Kaufman, M. Kellis, W. Gelbart, V.N. Iyer, et al. 2007. Evolution of genes and genomes on the *Drosophila* phylogeny. *Nature.* 450:203–218.

Cleveland, D.W., Y. Mao, and K.F. Sullivan. 2003. Centromeres and kinetochores: from epigenetics to mitotic checkpoint signaling. *Cell.* 112:407–421.

Collins, K.A., S. Furuyama, and S. Biggins. 2004. Proteolysis contributes to the exclusive centromere localization of the yeast Cse4/CENP-A histone H3 variant. *Curr. Biol.* 14:1968–1972.

Dalal, Y., H. Wang, S. Lindsay, and S. Henikoff. 2007. Tetrameric structure of centromeric nucleosomes in interphase *Drosophila* cells. *PLoS Biol.* 5:e218.

Dienemann, A., and F. Sprenger. 2004. Requirements of cyclin A for mitosis are independent of its subcellular localization. *Curr. Biol.* 14:1117–1123.

Dong, X., K.H. Zavitz, B.J. Thomas, M. Lin, S. Campbell, and S.L. Zipursky. 1997. Control of G1 in the developing *Drosophila* eye: rca1 regulates cyclin A. *Genes Dev.* 11:94–105.

Dunleavy, E.M., A.L. Pidoux, M. Monet, C. Bonilla, W. Richardson, G.L. Hamilton, K. Ekwall, P.J. McLaughlin, and R.C. Allshire. 2007. A NASP (N1/N2)-related protein, Sim3, binds CENP-A and is required for its deposition at fission yeast centromeres. *Mol. Cell.* 28:1029–1044.

Foltz, D.R., L.E. Jansen, B.E. Black, A.O. Bailey, J.R. Yates III, and D.W. Cleveland. 2006. The human CENP-A centromeric nucleosome-associated complex. *Nat. Cell Biol.* 8:458–469.

Fujita, Y., T. Hayashi, T. Kiyomitsu, Y. Toyoda, A. Kokubu, C. Obuse, and M. Yanagida. 2007. Priming of centromere for CENP-A recruitment by human hMis18alpha, hMis18beta, and M18BP1. *Dev. Cell.* 12:17–30.

Furuyama, T., Y. Dalal, and S. Henikoff. 2006. Chaperone-mediated assembly of centromeric chromatin in vitro. *Proc. Natl. Acad. Sci. USA.* 103:6172–6177.

Goshima, G., R. Wollman, S.S. Goodwin, N. Zhang, J.M. Scholey, R.D. Vale, and N. Stuurman. 2007. Genes required for mitotic spindle assembly in *Drosophila* S2 cells. *Science.* 316:417–421.

Grosskortenhaus, R., and F. Sprenger. 2002. Rca1 inhibits APC-Cdh1(Fzr) and is required to prevent cyclin degradation in G2. *Dev. Cell.* 2:29–40.

Hayashi, T., Y. Fujita, O. Iwasaki, Y. Adachi, K. Takahashi, and M. Yanagida. 2004. Mis16 and Mis18 are required for CENP-A loading and histone deacetylation at centromeres. *Cell.* 118:715–729.

Heeger, S., O. Leismann, R. Schittenhelm, O. Schraidt, S. Heidmann, and C.F. Lehner. 2005. Genetic interactions of separase regulatory subunits reveal the diverged *Drosophila* Cenp-C homolog. *Genes Dev.* 19:2041–2053.

Heun, P., S. Erhardt, M.D. Blower, S. Weiss, A.D. Skora, and G.H. Karpen. 2006. Mislocalization of the *Drosophila* centromere-specific histone CID promotes formation of functional ectopic kinetochores. *Dev. Cell.* 10:303–315.

Iwaki, T., M. Figuera, V.A. Ploplis, and F.J. Castellino. 2003. Rapid selection of *Drosophila* S2 cells with the puromycin resistance gene. *Biotechniques*. 35:482–484, 486.

Jansen, L.E.T., B.E. Black, D.R. Foltz, and D.W. Cleveland. 2007. Propagation of centromeric chromatin requires exit from mitosis. *J. Cell Biol.* 176:795–805.

Jaspersen, S.L., J.F. Charles, and D.O. Morgan. 1999. Inhibitory phosphorylation of the APC regulator Hct1 is controlled by the kinase Cdc28 and the phosphatase Cdc14. *Curr. Biol.* 9:227–236.

Jin, J., Y. Cai, B. Li, R.C. Conaway, J.L. Workman, J.W. Conaway, and T. Kusch. 2005. In and out: histone variant exchange in chromatin. *Trends Biochem. Sci.* 30:680–687.

Jorgensen, P.M., E. Brundell, M. Starborg, and C. Hoog. 1998. A subunit of the anaphase-promoting complex is a centromere-associated protein in mammalian cells. *Mol. Cell. Biol.* 18:468–476.

Kaspar, M., A. Dienemann, C. Schulze, and F. Sprenger. 2001. Mitotic degradation of cyclin A is mediated by multiple and novel destruction signals. *Curr. Biol.* 11:685–690.

Kiger, A.A., B. Baum, S. Jones, M.R. Jones, A. Coulson, C. Echeverri, and N. Perrimon. 2003. A functional genomic analysis of cell morphology using RNA interference. *J. Biol.* 2:27.

Kobor, M.S., S. Venkatasubrahmanyam, M.D. Meneghini, J.W. Gin, J.L. Jennings, A.J. Link, H.D. Madhani, and J. Rine. 2004. A protein complex containing the conserved Swi2/Snf2-related ATPase Swr1p deposits histone variant H2A.Z into euchromatin. *PLoS Biol.* 2:E131.

Konev, A.Y., M. Tribus, S.Y. Park, V. Podhraski, C.Y. Lim, A.V. Emelyanov, E. Vershilova, V. Pirrotta, J.T. Kadonaga, A. Lusser, and D.V. Fyodorov. 2007. CHD1 motor protein is required for deposition of histone variant H3.3 into chromatin in vivo. *Science.* 317:1087–1090.

Krogan, N.J., M.C. Keogh, N. Datta, C. Sawa, O.W. Ryan, H. Ding, R.A. Haw, J. Pootoolal, A. Tong, V. Canadien, et al. 2003. A Snf2 family ATPase complex required for recruitment of the histone H2A variant Htz1. *Mol. Cell.* 12:1565–1576.

Kurasawa, Y., and K. Todokoro. 1999. Identification of human APC10/Doc1 as a subunit of anaphase promoting complex. *Oncogene.* 18:5131–5137.

Kwon, M.S., T. Hori, M. Okada, and T. Fukagawa. 2007. CENP-C is involved in chromosome segregation, mitotic checkpoint function, and kinetochore assembly. *Mol. Biol. Cell.* 18:2155–2168.

Lehner, C.F., and P.H. O'Farrell. 1989. Expression and function of *Drosophila* cyclin A during embryonic cell cycle progression. *Cell.* 56:957–968.

Luk, E., N.D. Vu, K. Patteson, G. Mizuguchi, W.H. Wu, A. Ranjan, J. Backus, S. Sen, M. Lewis, Y. Bai, and C. Wu. 2007. Chz1, a nuclear chaperone for histone H2AZ. *Mol. Cell.* 25:357–368.

Lukas, C., C.S. Sorensen, E. Kramer, E. Santoni-Rugiu, C. Lindeneg, J.M. Peters, J. Bartek, and J. Lukas. 1999. Accumulation of cyclin B1 requires E2F and cyclin-A-dependent rearrangement of the anaphase-promoting complex. *Nature.* 401:815–818.

Machida, Y.J., and A. Dutta. 2007. The APC/C inhibitor, Emi1, is essential for prevention of rereplication. *Genes Dev.* 21:184–194.

Maddox, P.S., F. Hyndman, J. Monen, K. Oegema, and A. Desai. 2007. Functional genomics identifies a Myb domain–containing protein family required for assembly of CENP-A chromatin. *J. Cell Biol.* 176:757–763.

Mihaylov, I.S., T. Kondo, L. Jones, S. Ryzhikov, J. Tanaka, J. Zheng, L.A. Higa, N. Minamino, L. Cooley, and H. Zhang. 2002. Control of DNA replication and chromosome ploidy by geminin and cyclin A. *Mol. Cell. Biol.* 22:1868–1880.

Mizuguchi, G., X. Shen, J. Landry, W.H. Wu, S. Sen, and C. Wu. 2004. ATP-driven exchange of histone H2AZ variant catalyzed by SWR1 chromatin remodeling complex. *Science.* 303:343–348.

Moreno-Moreno, O., M. Torras-Llort, and F. Azorin. 2006. Proteolysis restricts localization of CID, the centromere-specific histone H3 variant of *Drosophila*, to centromeres. *Nucleic Acids Res.* 34:6247–6255.

Morgan, D.O. 2007. The Cell Cycle: Principles of Control. New Science Press, London. 297 pp.

Nickerson, H.D., A. Joshi, and D.J. Wolgemuth. 2007. Cyclin A1-deficient mice lack histone H3 serine 10 phosphorylation and exhibit altered aurora B dynamics in late prophase of male meiosis. *Dev. Biol.* 306:725–735.

Oegema, K., A. Desai, S. Rybina, M. Kirkham, and A.A. Hyman. 2001. Functional analysis of kinetochore assembly in *Caenorhabditis elegans*. *J. Cell Biol.* 153:1209–1226.

Okada, M., I.M. Cheeseman, T. Hori, K. Okawa, I.X. McLeod, J.R. Yates III, A. Desai, and T. Fukagawa. 2006. The CENP-H-I complex is required for the efficient incorporation of newly synthesized CENP-A into centromeres. *Nat. Cell Biol.* 8:446–457.

Scaerou, F., I. Aguilera, R. Saunders, N. Kane, L. Blottiere, and R. Karess. 1999. The rough deal protein is a new kinetochore component required for accurate chromosome segregation in *Drosophila*. *J. Cell Sci.* 112:3757–3768.

Schuh, M., C.F. Lehner, and S. Heidmann. 2007. Incorporation of *Drosophila* CID/CENP-A and CENP-C into centromeres during early embryonic anaphase. *Curr. Biol.* 17:237–243.

Takahashi, K., E.S. Chen, and M. Yanagida. 2000. Requirement of Mis6 centromere connector for localizing a CENP-A-like protein in fission yeast. *Science.* 288:2215–2219.

Topper, L.M., M.S. Campbell, S. Tugendreich, J.R. Daum, D.J. Burke, P. Hieter, and G.J. Gorbsky. 2002. The dephosphorylated form of the anaphase-promoting complex protein Cdc27/Apc3 concentrates on kinetochores and chromosome arms in mitosis. *Cell Cycle.* 1:282–292.

Zachariae, W., M. Schwab, K. Nasmyth, and W. Seufert. 1998. Control of cyclin ubiquitination by CDK-regulated binding of Hct1 to the anaphase promoting complex. *Science.* 282:1721–1724.

Erhardt et al., http://www.jcb.org/cgi/content/full/jcb.200806038/DC1

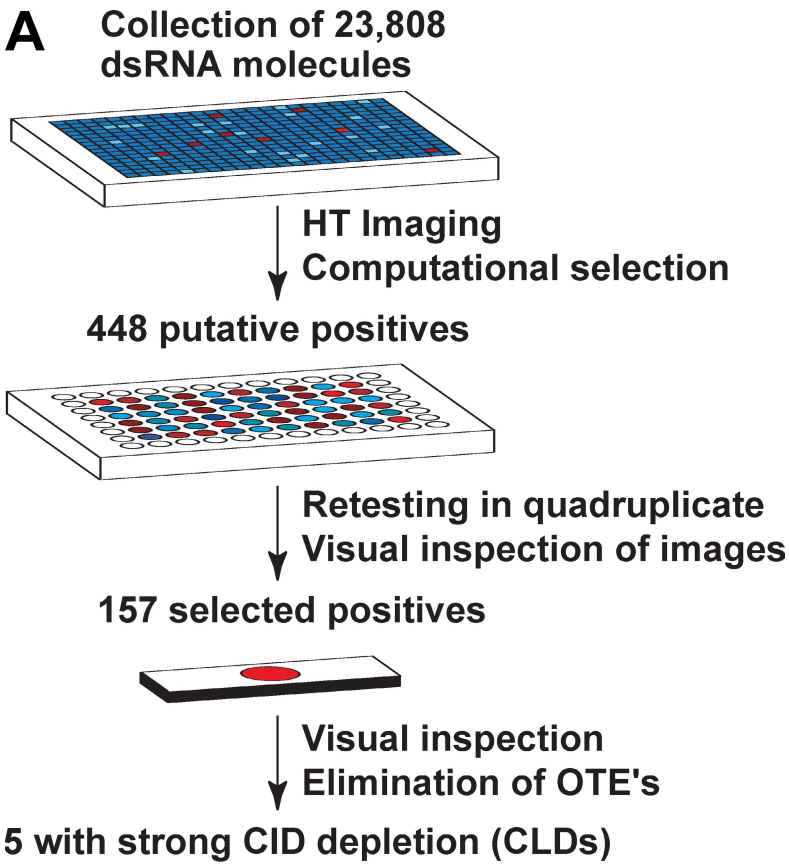

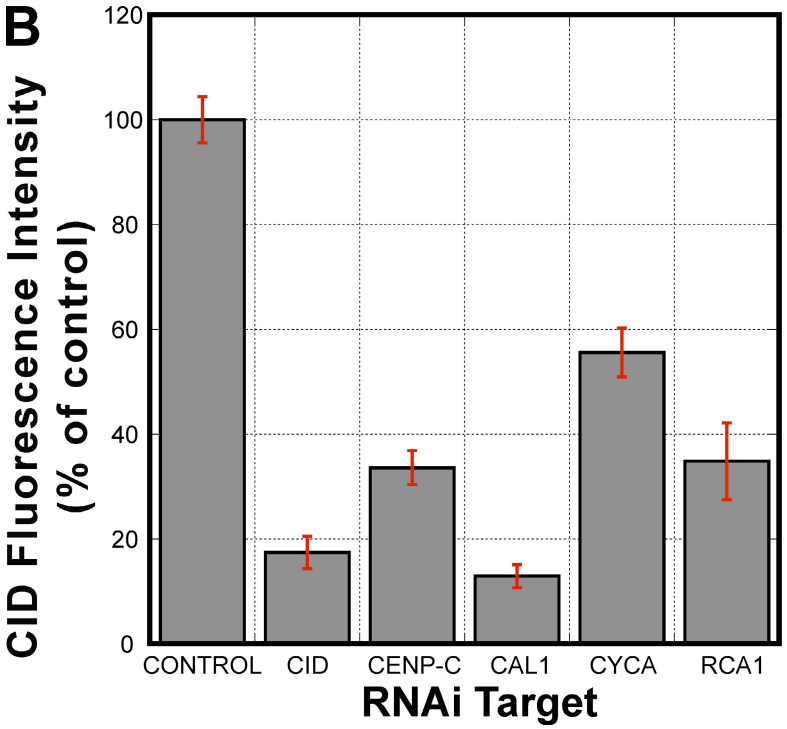

Figure S1. **Identification of genes required for CID localization by genome-wide RNAi screening.** (A) Schematic diagram of the screen to identify RNAi depletion targets that cause loss of CID staining. 23,808 genes and putative genes were depleted in a high throughput (HT) RNAi screen in *Drosophila* Kc167 cultured cells. 4 d after dsRNA addition, cells were fixed and stained for the centromeric histone CID, the heterochromatin protein HP1, and DNA (DAPI; Fig. 1 A). Automated imaging and computational analysis identified 448 putative candidate genes that specifically led to CID mislocalization after depletion in two independent screens. Visual inspection of the images yielded 157 selected positives. Five of those candidates (CLD genes 1–5) had the strongest effects on CID localization at the centromere, whereas the remaining 152 positives did not reproducibly give strong CID depletion. Four of the five selected positives were confirmed with dsRNAs covering different regions of the genes. The CLD5 (CG4329) phenotype could not be confirmed with alternative dsRNA and was therefore likely the result of an off-target effect (OTE; Echeverri, C.J., P.A. Beachy, B. Baum, M. Boutros, F. Buchholz, S.K. Chanda, J. Downward, J. Ellenberg, A.G. Fraser, N. Hacohen, et al. 2006. *Nat. Methods.* 3:777–779). (B) Quantification of CID fluorescence intensity at centromeres after dsRNA treatment for each CLD. $n = 4$; error bars represent SEM.

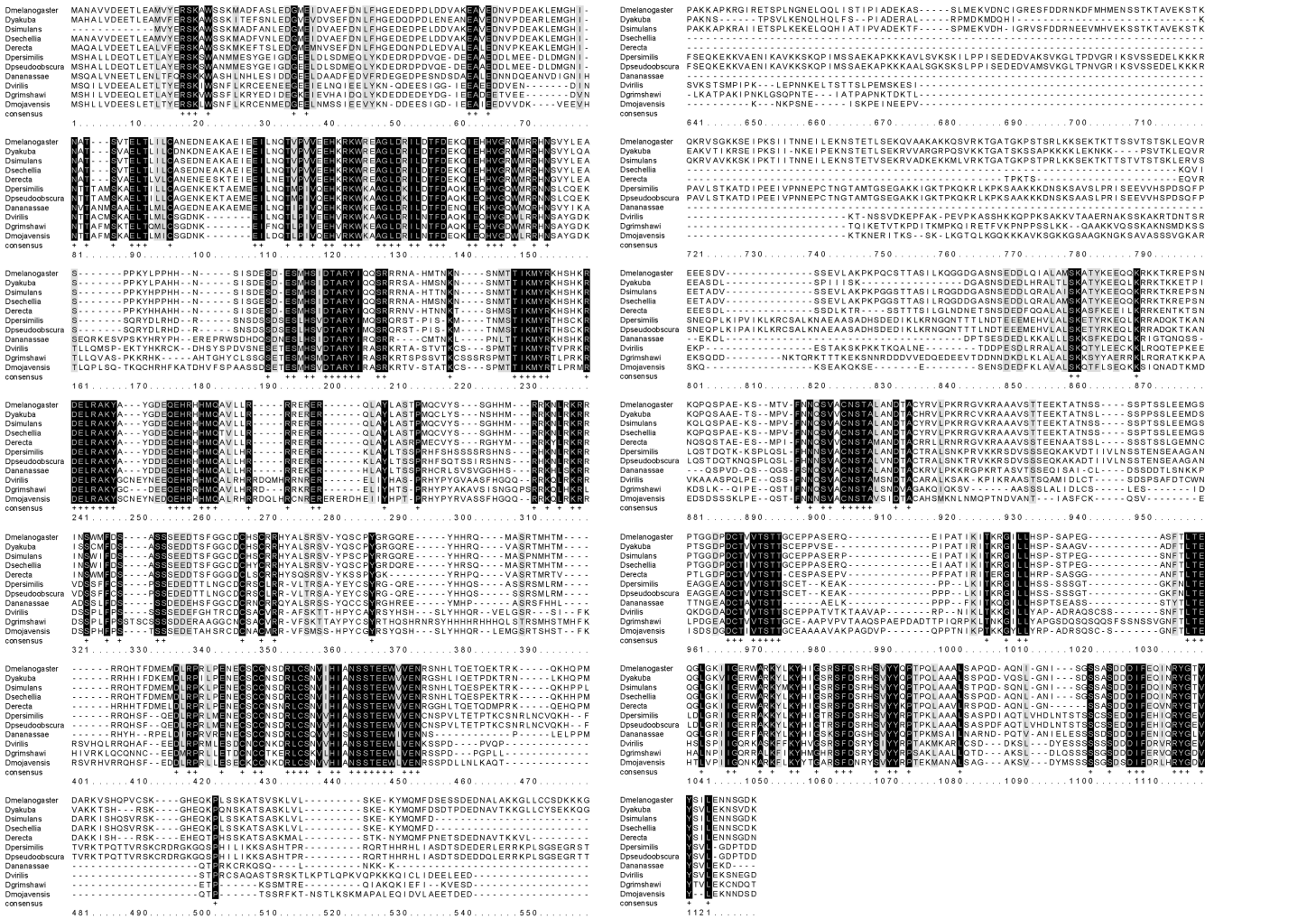

Figure S2. **Homologues of CAL1/CG5148 in other drosophilids.** Multiple sequence alignment of 11 CAL1 homologues from different drosophilid species (Lawrence Berkeley National Laboratory. 2006. Assembly/Alignment/Annotation of 12 Related *Drosophila* Species. University of California, Berkeley, Berkeley, CA. Available at: http://rana.lbl.gov/drosophila/caf1.html [accessed January 2006]). The species name is listed to the left. A plus sign in the consensus line represents residues that are identical between all 11 species, which is shown with a black background and gray letters. Conserved residues are represented with a gray background and black letters.

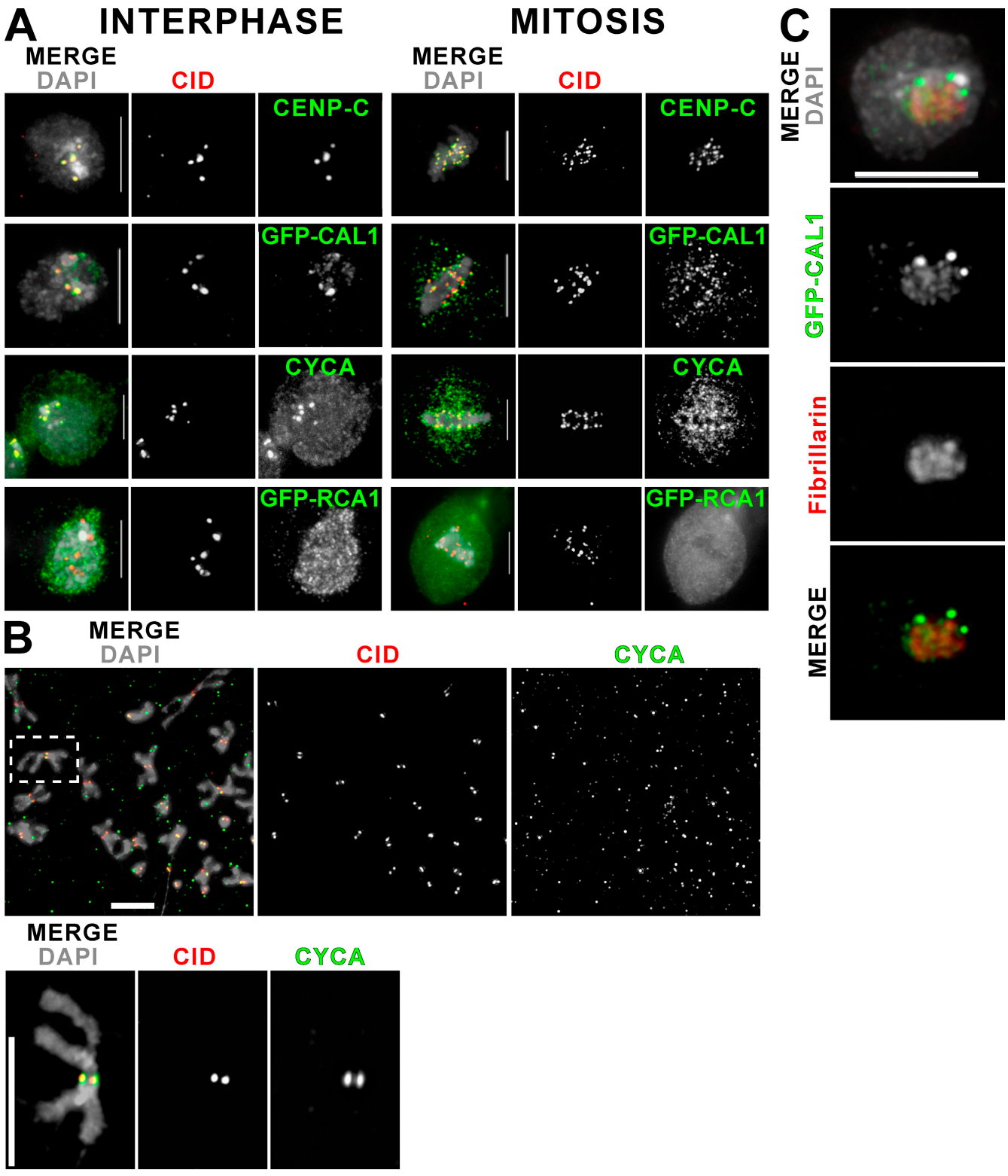

Figure S3. **Localization of CLDs in interphase and mitosis.** (A) *Drosophila* S2 cells were stained with antibodies recognizing CID (red), CENP-C, GFP, or CYCA (green), and DNA was stained with DAPI (gray). CENP-C is a constitutive inner kinetochore component that colocalized with CID at centromeres in interphase and mitosis (identified by tubulin staining; not depicted). GFP-CAL1 colocalized with CID in interphase and mitotic cells and is therefore a novel constitutive CENP. GFP-CAL1 also colocalized with the nucleolus in interphase cells (see C) and displayed a diffuse nuclear localization in mitosis. CYCA showed enrichment at the centromere in interphase and mitosis in addition to general cytoplasmic and nuclear staining. GFP-RCA1 localized to the nucleus in interphase cells with no enrichment at centromeres and was present at low levels throughout mitosis. (B) Metaphase chromosome spreads of S2 cells were stained with anti-CID (red) and anti-CYCA (green) antibodies. The strongest CYCA signal at this cell cycle stage colocalized with CID to the centromere (see Fig. 1 B and Video 4). (C) S2 cells expressing GFP-CAL1 were stained with anti-GFP (green) and antifibrillarin (red) antibodies, demonstrating extensive colocalization of CAL1 with the nucleolus and association of centromeres with the nucleolar periphery (DAPI, gray). The nucleolar localization of GFP-CAL1 is intriguing given the identification of a physical association between CENP-A and a nucleolar component (nucleophosmin; Foltz, D.R., L.E. Jansen, B.E. Black, A.O. Bailey, J.R. Yates III, and D.W. Cleveland. 2006. *Nat. Cell Biol.* 8:458–469). Inset shows magnification of the image. Bars, 5 µm.

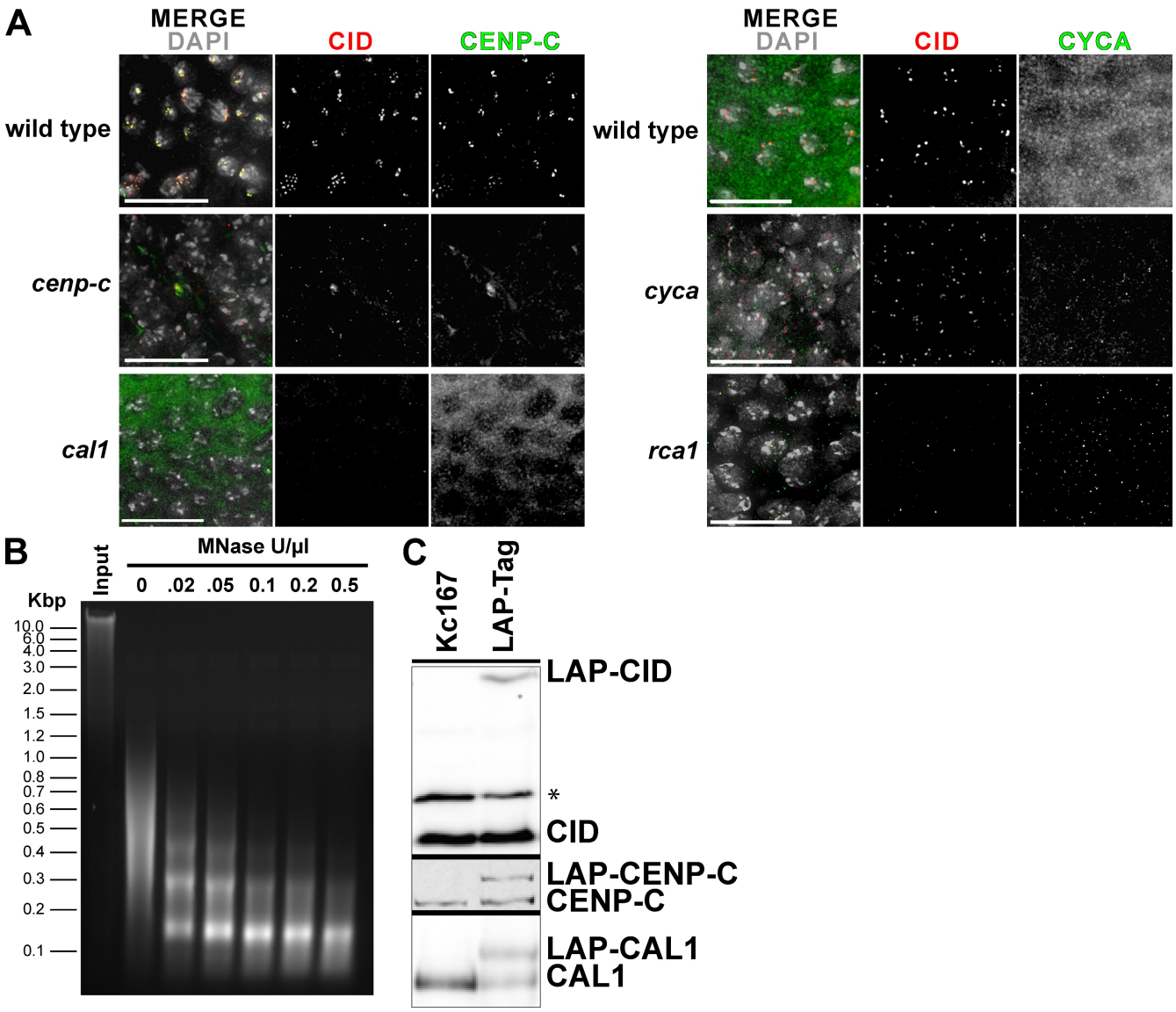

Figure S4. **Loss of CID localization in CLD mutant embryos.** (A) Wild-type embryos display overlapping CID (red) and CENP-C (green) localization to the centromere. CID levels at centromeres were highly reduced in *cenpC*, *cal1*, *cycA*, and *rca1* mutant embryos. CENP-C was dispersed from the centromere in CAL1 mutant embryos (left), which is similar to results in CAL1-depleted cultured cells (Fig. 3 A). The level of CYCA (green) in *rca1* and *cycA* mutants was also highly reduced (right). (B) Fragmentation of Kc167 cell chromatin. The digestion of chromatin with 0.1 U/µl micrococcal nuclease followed by sonication yields primarily mono- and dinucleosomal-length chromatin fragments. DNA molecular weight markers are indicated at the left. The first lane is the untreated input Kc167 cell chromatin, the second lane is sonicated Kc167 cell chromatin, and the subsequent lanes are chromatin digested with micrococcal nuclease in increasing concentrations followed by sonication. LAP tag purifications were performed with chromatin treated with 0.1 U/µl MNase followed by sonication. (C) Expression level of LAP-tagged CLD proteins compared with endogenous CLD proteins. Whole cell extract from parent Kc167 cells or stable cell lines expressing LAP-CID (60 kD; top), LAP–Cenp-C (190 kD; middle), or LAP-CAL1 (150 kD; bottom) were Western blotted with α-CID (31 kD), CENP-C (160 kD), or CAL1 (120 kD) antiserum. All fusion proteins are expressed at or below the level of the endogenous protein. A cross reacting band in the CID Western blot is indicated with an asterisk. Black lines indicate that intervening lanes have been spliced out. Bars, 10 µm.

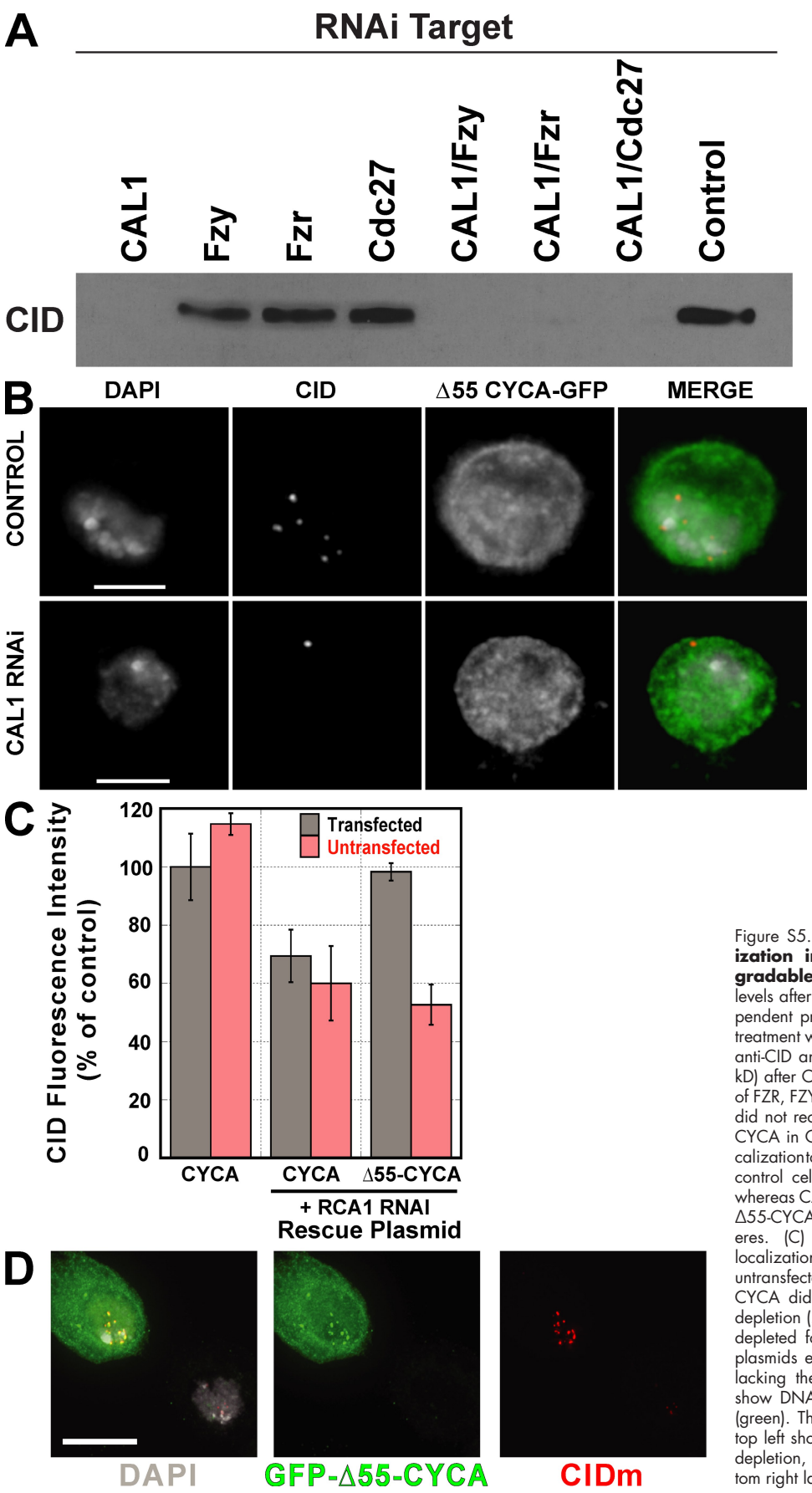

Figure S5. **Rescue of centromeric CID localization in RCA1-depleted cells by nondegradable CYCA.** (A) The reduction of CID protein levels after CAL1 depletion is not caused by APC-dependent proteolysis. Extracts from cells depleted by treatment with dsRNA (RNAi target) were blotted with anti-CID antibodies. The reduction in CID levels (31 kD) after CAL1 depletion is not restored by depletion of FZR, FZY, or the APC subunit CDC27. Control cells did not receive dsRNA. (B) Expression of GFP–Δ55-CYCA in CAL1-depleted cell does not rescue CID localization to centromeres. GFP–Δ55-CYCA–expressing control cells (top) display normal CID localization, whereas CAL1-depleted control cells expressing GFP–Δ55-CYCA (bottom) fail to localize CID to centromeres. (C) Quantification of the rescue of CID localization by GFP–Δ55-CYCA in transfected versus untransfected cells. Wild-type (degradable) GFP-CYCA did not rescue CID localization after RCA1 depletion (n = 4; error bars represent SEM). (D) Cells depleted for RCA1 by RNAi were transfected with plasmids expressing GFP-CYCA or GFP–Δ55-CYCA lacking the cyclin destruction box. The left panels show DNA (gray), CID (red), and GFP–Δ55-CYCA (green). The GFP–Δ55-CYCA–transfected cell at the top left shows rescue of CID localization after RCA1 depletion, whereas the untransfected cell at the bottom right lacks CID at the centromere. Bars, 15 μm.

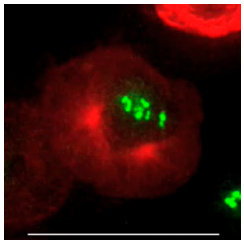

Video 1. **GFP-CID and mCherry-tubulin.** This video shows a mitotic S2 cell expressing GFP-CID and mCherry-tubulin. GFP-CID localizes at centromeres throughout mitosis. Stills are shown in Fig. 1 B. Bar, 15 µm.

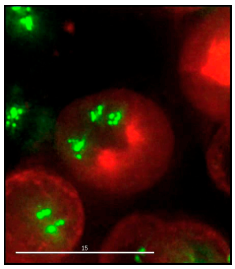

Video 2. **GFP–CENP-C and mCherry-tubulin.** This video shows a mitotic S2 cell expressing GFP–CENP-C and mCherry-tubulin. GFP–CENP-C localizes at centromeres throughout mitosis. Stills are shown in Fig. 1 B. Bar, 15 µm.

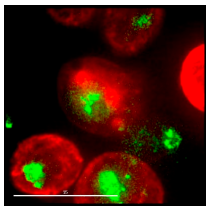

Video 3. **GFP-CAL1 and mCherry-tubulin.** This video shows a mitotic S2 cell expressing GFP-CAL1 and mCherry-tubulin. GFP-CAL1 localizes at centromeres throughout mitosis. The fluorescence intensity of GFP-CAL1 appears to decrease during metaphase and increase again in telophase. Stills are shown in Fig. 1 B. Bar, 15 µm.

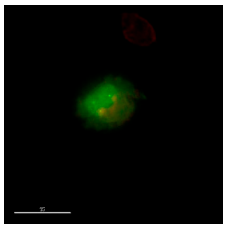

Video 4. **GFP-CYCA and mCherry-tubulin.** This video shows the localization of GFP-CYCA (expressed under the control of the endogenous CYCA promoter) during mitosis in S2 cells. GFP-CYCA localizes diffusely in the nucleus and accumulates at centromeres in prometaphase. After nuclear envelope breakdown, the diffuse GFP-CYCA signal decreases, and the centromeric staining becomes more visible. The GFP-CYCA signal decreases dramatically in anaphase, which is presumably caused by APC-dependent proteolysis. Bar, 15 µm.

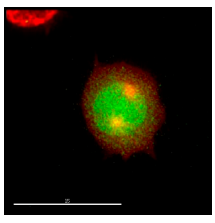

Video 5. **GFP-RCA1 and mCherry-tubulin.** This video shows the localization of GFP-CYCA during mitosis in S2 cells. GFP-RCA1 levels are high and diffuse within the nucleus before mitosis. Upon nuclear envelope breakdown, the GFP-RCA1 signal becomes more diluted, and it disappears in anaphase and finally reappears during cytokinesis when the nuclear envelope is reformed. Bar, 15 µm.

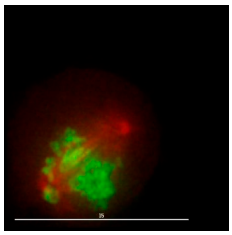

Video 6. **Control for RNAi experiments.** This video shows that untreated S2 cells expressing H2B-GFP and mCherry-tubulin divide normally. The chromosomes condense and align at the metaphase plate, and sister chromatids are pulled toward opposite poles in anaphase as the spindle elongates. Chromosome segregation is completed timely and accurately. Stills are shown in Fig. 2. Bar, 15 µm.

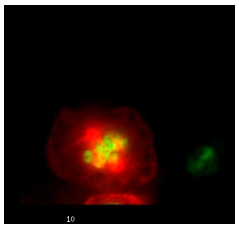

Video 7. **CID RNAi.** This videos shows S2 cells expressing H2B-GFP and mCherry-tubulin undergoing mitosis after CID depletion. CID depletion results in chromosomes that are unable to attach to the spindle or move, and the chromosomes remain stalled in metaphase. The spindle elongates prematurely, and mitosis does not complete. Stills are shown in Fig. 2. Bar, 15 µm.

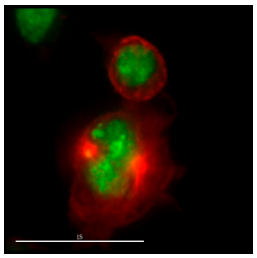

Video 8. **CENP-C RNAi.** This video shows S2 cells expressing H2B-GFP and mCherry-tubulin undergoing mitosis after CENP-C depletion. This video shows cells displaying chromosome misalignment, severe spindle formation defects, and failure of sister chromatid separation. Cytokinesis can proceed without proper chromosome segregation, resulting in a "cut" phenotype and severe aneuploidy. Stills are shown in Fig. 2. Bar, 15 µm.

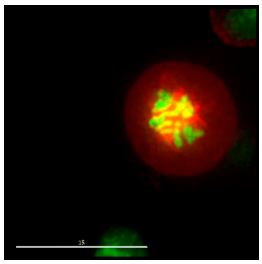

Video 9. **CAL1 RNAi.** This video shows S2 cells expressing H2B-GFP and mCherry-tubulin undergoing mitosis after CAL1 depletion. Cells are unable to form a functional mitotic spindle, and multipolar spindles are often observed. Chromosomes fail to congress correctly and are hypercondensed, and cytokinesis results in uneven segregation. Stills are shown in Fig. 2. Bar, 15 µm.

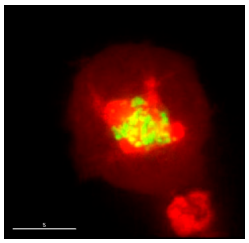

Video 10. **CYCA RNAi.** This video shows S2 cells expressing H2B-GFP and mCherry-tubulin undergoing mitosis after CYCA depletion. Cells show severe mitotic defects, including defective spindles and missegregation of chromosomes. Most cells stop dividing after 2–3 d of RNAi treatment, and many do not progress beyond prometaphase (this video shows day 2 after RNAi treatment). The cytokinesis defect giving rise to multinucleated cells in this video is the most distinct phenotype compared with CID, CENP-C, or CAL1 depletion. Stills are shown in Fig. 2. Bar, 15 µm.